INVESTIGATION OF THE KINETCIS AND MECHANISMS OF THE INACTIVATION OF PTP-SHP2 BY PEROXYCARBONATE AND PHYTOCHEMICALS

A Thesis

presented to

the Faculty of the Graduate School

at the University of Missouri-Columbia

In Partial Fulfillment

of the Requirements for the Degree

Master of Science

---

by

SARAH LEWIS

Dr. Kent Gates, Thesis Supervisor

May 2012

The undersigned, appointed by the dean of the Graduate School, have examined the thesis entitled

INVESTIGATION INTO THE KINTECS AND MECHANISM OF THE INACTIVATION OF PTP-SHP2 BY PEROXYCARBONATE AND PYTOCHEMICALS

presented by Sarah Marie Lewis

a candidate for the degree of Master of Science

and hereby certify that, in their opinion, it is worthy of acceptance.

Dr. Kent Gates

Dr. John Tanner

Dr. Thomas Reilly

I would like to dedicate this work to my family, for all their love and support, and to my friends for keeping me sane.

I would like to also thank the 2 greatest puppies in the world: Raider and Swizzle

Most of all I would like to dedicate this to my father, Thomas Thayer Lewis,

for being my biggest fan, I love you dad.

ACKNOWLEDGEMENTS

My journey through graduate school has allowed me to enjoy the instruction of several people; I would like to acknowledge the following for helping me get this far.

I would like to thank my advisor, Kent Gates, for teaching to me to ignore the car wrecks. As Dr. Gates so eloquently put he “is been both the wind under my wings and the anchor that drags me down”.

I wish to thank my committee members; Dr. Tanner and Dr. Reilly, for taking the time to teach me over the past 3 years and for their guidance.

Lastly, I need to thank the Gates Group. Every member past and present has had a huge impact on my research career. I thank you all for being my adopted family while I was here and most of all I thank you guys for helping me learn ‘big words’, for being my dictionary, pronunciation guide, and thesaurus.

I would also like to thank Jerry Brightwell for knowing the answers to every question I have, and Mary Laney for being so helpful.

TABLE OF CONTENTS

LIST OF TABLES

Page

LIST OF FIGURES

Page

LIST OF SCHEMES

Page

1.1 Introduction to Protein Tyrosine Phosphatases

Protein phosphatases were once considered simple housekeeping enzymes, but it is now known they operate in tandem with protein kinases during the regulation of the phosphorylation state of tyrosine residues in proteins (Figure 1.1).[1] Protein tyrosine kinases (PTKs) phosphorylate tyrosine residues and protein tyrosine phosphatases (PTPs) remove inorganic phosphate from the phosphotyrosine residues.

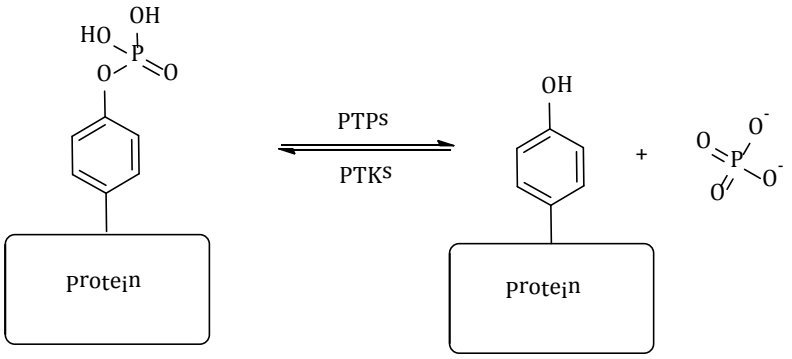

Figure 1.1 PTPs and PTKs work in tandem to control the phosphorylation state of tyrosine residues.[1]

Regulation of the phosphorylation state of tyrosine residues and their associated signaling pathways serves a key role in the progression of many mammalian diseases.[2-10] PTPs and PTKs function as an 'on/off' switch for mammalian signaling

pathways and thus the downstream signaling that occurs. Kinases control the magnitude of the signal; whereas phosphatases control the duration of response.[9]

These cysteine dependent enzymes are part of the super-family of enzymes named phosphatases, which includes PTPs. This 100 member family[9], is responsible for many cellular signaling processes, but PTPs dephosphorylate phosphotyrosine residues during the regulation of signaling responses.[9] The protein tyrosine phosphatases are defined by a signature active site motif VHCXGXGR(T/S),[11] and are divided into three main subgroups: the classical phosphatases, dual specificity phosphatases, and the low molecular weight phosphatases.[9] The classical phosphatase group is further divided into two subgroups; transmembrane, receptor-like PTPs (RPTPs) and non-transmembrane, cytoplasmic PTPs.[9] The non-transmembrane PTPs are characterized by regulatory sequences that flank the catalytic domain[9], aiding in the control of catalytic activity, which will be discussed in further detail in the following section.

1.2 Active Site Structure of PTPs

As previously reported in section 1.1, PTPs share sequence and structural similarities.[11] Though there are ten conserved motifs within this enzyme family[11], this work will focus on four specific domains (Figure 1.2) that are involved in the catalytic

mechanism utilized by PTPs. This section focuses on the structural characteristics that are important to the biological function of PTPs.

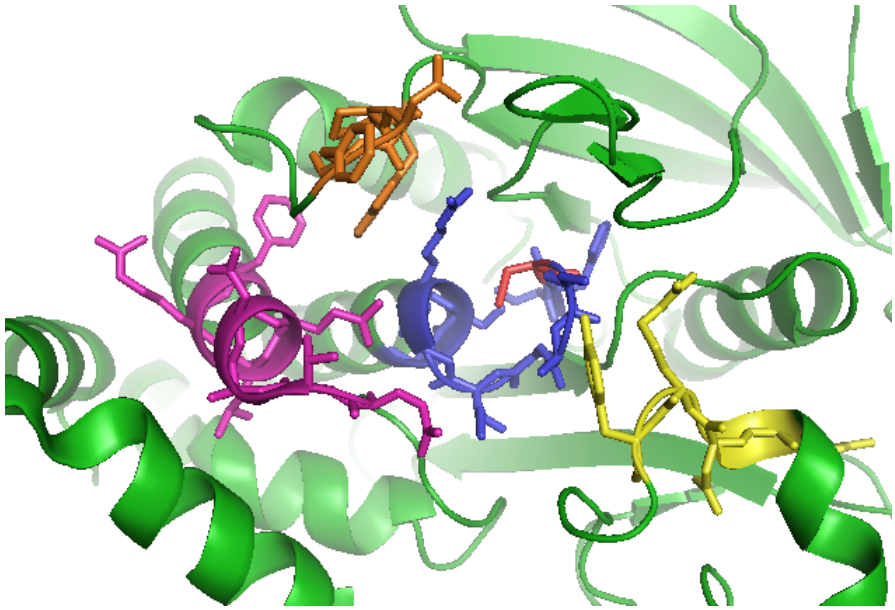

Figure 1.2 Close up of PTP1B with the active site residues colored blue, P-Loop colored yellow, WPD Loop colored orange, the Q-Loop purple and cysteine 215 shown in red.

A stated previously (Section 1.1), the active site of PTPs have a signature sequence of VHCSXGXR(T/S)G for residues 213 – 223 (Fig 1.3). This sequence is described using the prototypical numbering system of Protein Tyrosine Phosphatase 1B (PTP1B), which is the best characterized PTP of the family. The pK_a of the catalytic cysteine (Cys 215) is 5.5 and at physiological pH this cysteine is a thiolate ion, which will be discussed in further detail in section 1.5. Due to Cys 215's close proximity to the main chain amide groups in the active site, it is able to hydrogen bond with the side chains of Arg 221 and Ser 222, which help stabilize the thiolate ion.[11] (Figure 1.3) The active site

motif is also able to assist in substrate binding and the stabilization of the phospho-enzyme intermediate.[11]

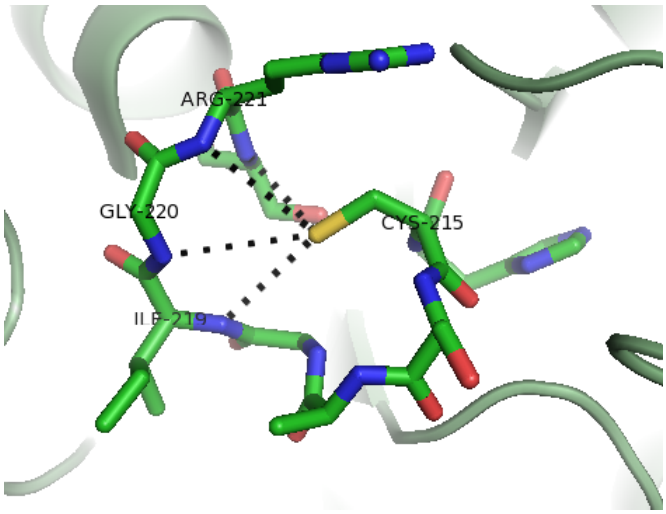

Figure 1.3 PyMOL rendering of the active site of PTPs shown with hydrogen bonding of Cys 215 to other residues that aid in the stablization of the thiolate ion.

The phosphotyrosine recognition loop (P-Loop) is comprised of the residues KNRY (Lys 43-Tyr46), and confers depth to the active site.[11] This allows for selectivity of phosphotyrosine by excluding shorter phosphoserine and phosphothreonine residues from the active site.

The WPD loop is the catalytic site surface loop, consisting of the residues WPDXGXP (Trp179-Phe182). This portion of the structure includes a general acid/base, (Asp181), two proline residues and a glycine residue. These structural features form the hinge/bend region of the loop, which is critical for the structure and function of the

WPD loop. This loop is capable of moving significant movement (7Å),[12] trapping the substrate in the active site. After completion of the catalytic cycle, the WPD loop opens and releases inorganic phosphate. Of the residues in the WPD-loop, Trp179 and Arg221 aid in the catalysis of the substrate, and Asp181's proximity to the bound substrate donates a proton to the phenolate leaving group.[11]

The Q-loop is comprised of residues 262-269, with two glutamine residues and two arginine residues *N*-terminal to the loop that form crucial hydrogen bonding interactions with residues of the PTP-loop at its amide backbone. Glutamine 262 positions a water molecule which is involved in the second step of catalysis of the phosphocysteine intermediate. The two glutamine residues restrict phosphoryl transfer from the phosphoenzyme intermediate to a water molecule, or other nucleophilic acceptors.[11]

1.3 The Catalytic Mechanism of PTPs

The catalytic mechanism has been well established for PTPs, and can be thought of in a simple five step manner. The first step is substrate binding to the active site and the WPD loop moves to a closed position. Second, the thiolate residue (Cys 215) attacks the phosphoryl group of the substrate and yields a phosphoryl cysteine[13] intermediate.

Third, Asp 181 donates hydrogen to a phenolate ion[14] which is the leaving group. Fourth, Asp 181 again helps by activating a water molecule to attack the posphoryl cysteine, and lastly, inorganic phosphate is released to regenerate active enzyme (Scheme1.1)[13-14].

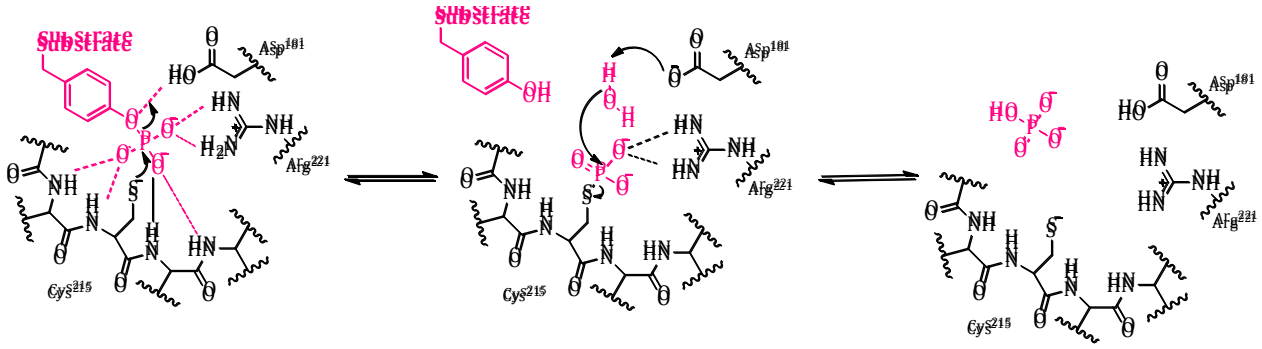

Scheme 1.1 The PTP catalytic mechanism, using PTP1B numbering for the amino acids.

1.4 Introduction to Reactive Oxygen Species

Reactive oxygen species (ROS) play important physiological roles in the cell. They are implicated in the damage due to ageing[15-16], the complications of diabetes,[17] the pathology of cancer[7], and cardiovascular diease.[15] It has been noticed that small amounts of ROS are released, serving as a secondary messenger aiding in cellular response during the insulin signaling cascade.[12,17-18]

Chapter 1: Introduction to Protein Tyrosine Phosphatases

NADPH oxidase enzymes (Nox) are a source of rapid generation of ROS during the insulin cascade.[17] Nox4 is a predominate NADPH oxidase catalytic subunit homolog to Nox2 that is expressed in adipose tissue.[18] In the 1970s, insulin was shown to cause the generation of hydrogen peroxide in adipocytes[18] by the activation of a plasma membrane enzyme (such as Nox) which results in the downstream production of hydrogen peroxide.[16,19] Nox catalyzes the reduction of oxygen to super oxide radical via reaction 1.[19] The resulting superoxide cannot react with thiols; therefore, it is converted to hydrogen peroxide in the cell by superoxide dismutase (SOD).

$$2\ O_2 + NADPH \rightarrow 2O_2\cdot^- + NADP^+ + H^+ \qquad (1)$$

Nox4 was found in mature adipocytes, and there is evidence of Nox4 playing a role in the insulin induced formation of hydrogen peroxide.[20] When Nox4 knockout cells were grown, there was noticeable inhibition of insulin signaling , tyrosine phosphorylation of the insulin receptor, its protein IRS-1, and glucose uptake.[17,18] Nox4 is involved in the generation of hydrogen peroxide by insulin stimulation of differentiated 3T3-L1 adipocytes.[20] Changing the expression of Nox4 affects both early and late events in the insulin signal transduction pathway.[18] This furthered the theory that Nox4 should be seen as a link between the insulin receptor and ROS generation that increases insulin signal transduction due to the oxidative inhibition of cellular PTPases like PTP1B.[17]

1.5 Redox Regulation of PTPs

Due to their critical role in signal transduction, PTPs are important targets of H_2O_2 production within the cell. PTP1B activity is dependent upon the oxidation state of the catalytic cysteine (Cys215), which forms a phospho-enzyme intermediate necessary for catalytic activity.[17] Because the pK_a of the catalytic cysteine (pK_a=5.5) is relatively low when compared to a normal sulfhydrol group(RSH-) (pK_a=8.5) [17], it is sensitive to oxidation at physiological pH due to its presence as a thiolate ion (RS-) . This allows for the catalytic cysteine of PTPs to be readily oxidized by ROS, such as hydrogen peroxide, even in the presence of high glutathione concentrations. Scheme 1.3 illustrates the inactivation of the catalytic cysteine by hydrogen peroxide to the unstable sulfenic acid.

Previous work has shown that three PTPs (PTP1, LAR, and VHR) from the PTP family were inactivated with high micromolar concentrations of hydrogen peroxide (900 μM) resulting in calculated rate constants of 9.01 ± 0.1 $M^{-1}sec^{-1}$, 17.9 ± 1.3 $M^{-1}sec^{-1}$, and 14.0 ± 3.1 $M^{-1}sec^{-1}$, respectively.[3] Further work was performed to determine if the hydrogen peroxide was reacting with the active site cysteine or other cysteine residues within the proteins. It was determined that thiol of the active cysteine was in fact being oxidized during the inactivation of these PTPs.[3,21,12] This was elucidated through the

active site cysteine being replaced with a serine and no measurable activity being observed.

Denu and Tanner[3] investigated the reversibility of hydrogen peroxide inactivation on the active site cysteine through the use of thiols to recover activity of the oxidized PTPs. It was determined that dithiothreitol (DTT), β-mercaptoethanol, reduced glutathione, and cysteine were all able to regenerate the activity of the oxidized PTPs.[3] It was also observed that recovery of the active enzyme was faster with DTT, which led to the conclusion that the active site cysteine required two equivalents of thiol to fully recover activity.

To determine the chemical structure of the oxidized cysteine (Scheme 1.1), a PTP was oxidized with hydrogen peroxide for 10 minutes and then treated with thiols at various times from 10 to 180 minutes.[3]

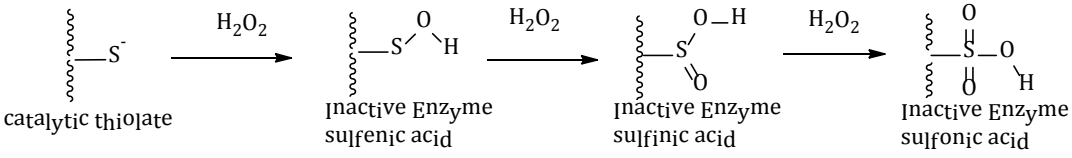

Scheme1. 2 Oxidation of PTP cysteine thiolate by hydrogen peroxide.

Since the enzyme was able to recover most of its activity, it was assumed the cysteine residue had been oxidized to its sulfenic acid form (R-SOH) rather than the unrecoverable sulfinic ($R\text{-}SO_2H$) or sulfonic acid ($R\text{-}SO_3H$) forms[3,22](Schemes 1.2 and 1.3).

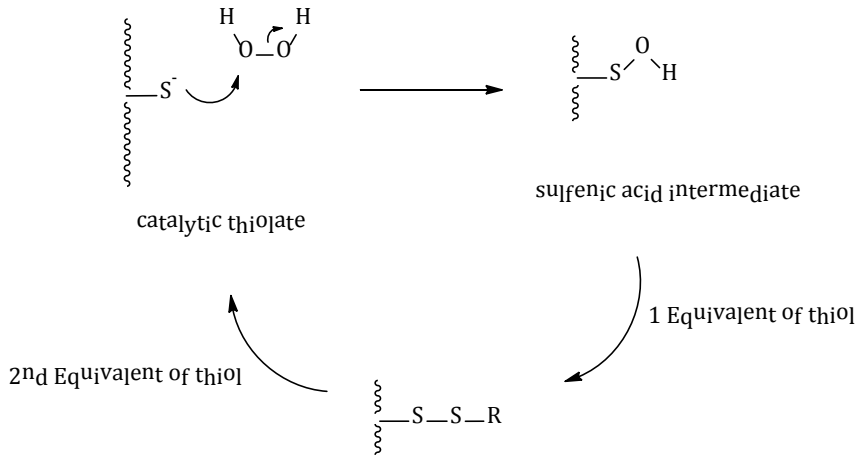

Scheme 1.3 Proposed mechanism for the reversible inactivation of PTPs.

Originally it was proposed that PTPs were oxidized to a sulfenic acid intermediate[13], which was considered stable due to the local environment of the active site pocket. It was later determined the sulfenic acid was converted to an sulfenyl amide (Scheme 1.4).[3,12,17,21] The formation of the sulfenyl amide occurs when the sulphur atom of the catalytic cysteine becomes covalently bonded to the main chain nitrogen from its neighboring residue. This sulphenyl amide causes large structural changes in the

conformation of the active site pocket, which in turn protects the catalytic cysteine from being over oxidized to the irreversible sulfonic form.[12]

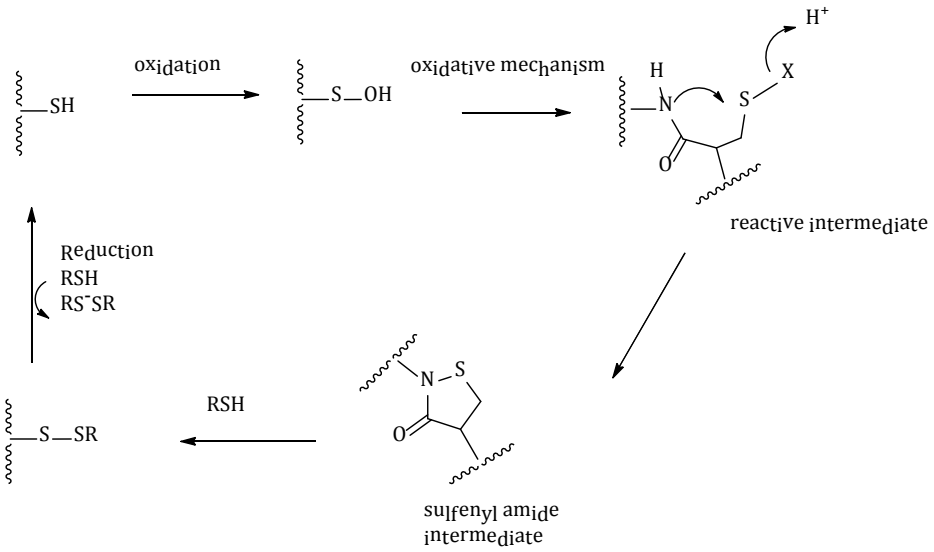

Scheme 1.4 Mechanism for the formation of sulphenyl amid intermediate during oxidation of PTPs with ROS followed by the reduction by thiol to return active enzyme.[21]

1.6 Crystal Structures of PTP Regulation

The presence of the sulfenyl amide of PTP was determined during crystallographic soaks of PTP1B performed by H. Jhoti and associates[21]. Significant electron density was observed close to the catalytic cysteine which could be explained by a covalent bond between the sulphur atom of Cys215 and the main chain nitrogen of the neighboring serine residue (Ser216).[12,21]

The sulfenyl amide bond length was determined to be 1.7 Å, which gave a puckered five-member ring that had not previously been observed in proteins. Due to the presence of this sulfenyl amide, the active site pocket changed into a distorted form, which included the shift of the pTyr-binding site that aided in the stabilization of the sulfenyl amide by hydrophobic interactions with the side chain Ile 219.[21] The P-loop takes on a more exposed conformation and loses hydrogen bonding capabilities with hydroxyl groups from Tyr46 and Ser216 which normally anchor the pTyr-loop in native PTP1B. (Figure 1.4) This exposed form is stabilized by water molecules and interactions with Asp48. Finally, Gly262 from the Q-loop is moved out of the binding pocket changing its orientation

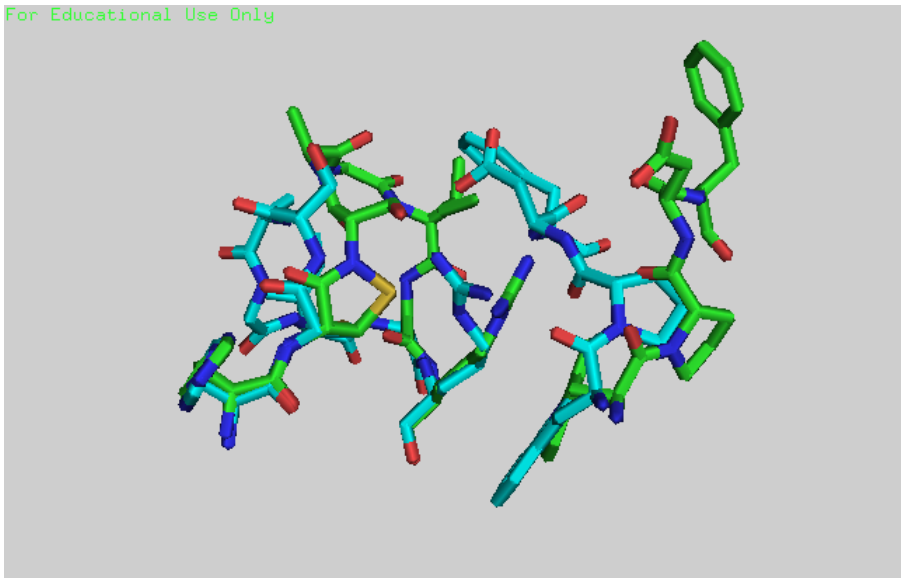

Figure 1.4 PyMOL overlay of the P-loop and Q-loop of open (colored blue) and closed (colored green) PTP active site with sulfenyl amide.

1.7 Src Homology 2 Domain Containing PTPs

Much of the work described here examines the inactivation of a particular human PTP enzyme known as SHP2. Therefore, a brief overview of the structure and function of this enzyme is provided.

Src homology phosphatases (SHPs) contain both a classical PTP domain and a SH2 domain.[19,23] SHP2 is a PTP that contains two SH2 domains at its *N*-teminus (*N*-SH2 and *C*-SH2), a PTP domain, and a *C*-terminal tail.[2,23-26](Figure. 1.5) Current research is largely focused on the PTP domain of SHP2, with structural information about its control of the utmost importance.

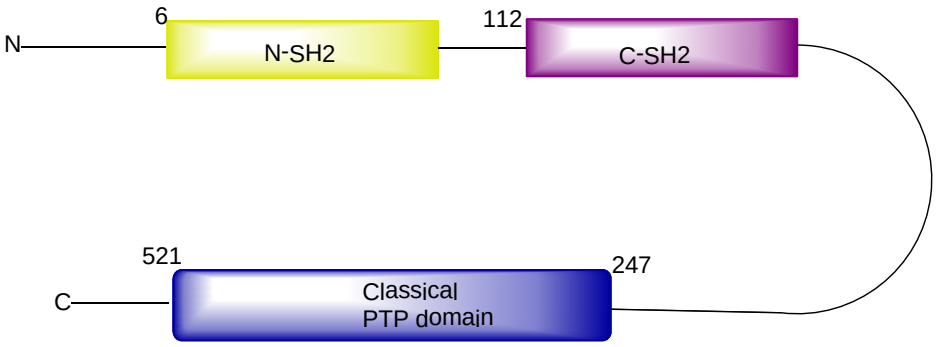

Figure 1.5 Schematic drawing of *N*-SH2 domain (shown in yellow), the *C*-SH2 domain (shown in purple) and the PTP domain (shown in blue) for SHP2.

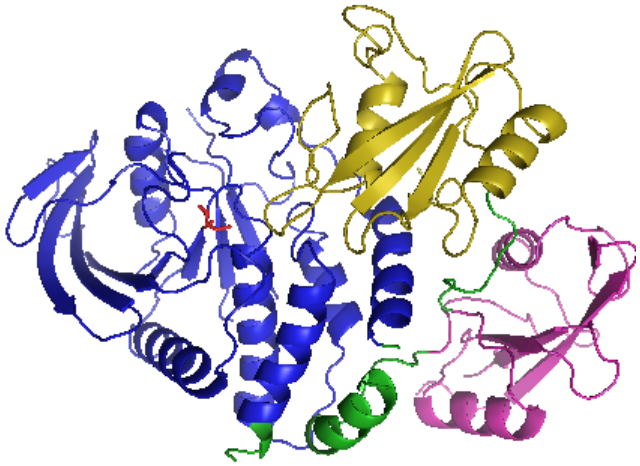

Figure 1.6 PyMOL of SHP2 with the *N*-SH2 domain shown in yellow, the *C*-SH2 domain colored purple, and the PTP domain shown in blue with the catalytic cysteine colored red.

The *N*-SH2 domain was determined to suppress PTP activity by intermolecular interactions with residues on the backside loop of the *N*-SH2 domain and the catalytic surface of the PTP domain.[2,23,26] (see Figure 1.6) SHP2 was found to interact with several ligand-activated receptor PTKs (R-PTKs), this means that interaction is mediated through recognition of a pTyr on a receptor by the SH2 domain (*N*-SH2).[24] Phosphorylated tyrosine residues on R-PTKs, cytokine receptors, and scaffolding adaptors recruit SHP2, bind to the self inhibiting *N*-SH2 domain,[24] permitting the exposure of the catalytic PTP domain and allow catalytic activation of SHP2.[2] The SH2 domain thus has two functions; the first is to direct the PTP to its substrate and the

second is to control the rate of catalysis with the rate of phosphorylation of a tyrosine on its domain.[24] In the basal state, the SH2 domain blocks the PTP domain [25],which in short serves as a 'molecular switch' for PTP activity.[2,19]

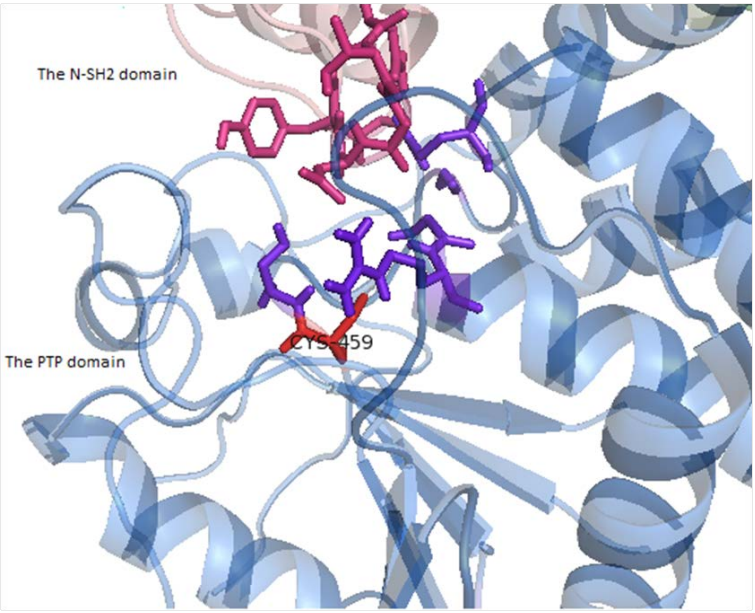

Figure 1.7 PyMOL close-up of SHP2, with its N-SH2 domain colored purple and the its PTP domain shown in blue, with its catalytic cysteine shown in red.

1.8 PTP-SHP2's Role In the Cell

PTPs can have either a positive (signal enhancing) or negative (signal diminishing) role in signal transduction pathways[25]. SHP2 is a positive regulator of cell signaling, downstream of growth factor, cytokine and extracellular matrix receptors.[25] This serves

an important role in regulating cell growth, transformation, differentiation and migration, since SHP2 is required for Ras activation in most of these pathways.[25,27]

Ras is part of the Ras sub-family of small GTPases that participate in signal transduction. Activation of Ras signaling allows for cell growth, differentiation, and determines cell survival. SHP2 has been connected to Ras signaling by studies involving juvenile myelodysplasic leukemia (JMML) and Noonan Syndrome (NS), where 35% of JMML patients, and 50% of NS patients have an activated mutation of SHP2.[25] One of the associated mutations of SHP2 occurs between the *N* and *C*-SH2 domains causing the formation of a 'kink'[23] on the *N*-SH2 domain preventing the auto inhibitory action of this domain with the PTP domain. All JMML cases without SHP2 mutations have an activating Ras mutation that inactivates the neurofibromatosis type 1 (NF1) gene, which aids in the control of Ras.[27-28]

As shown in Figure 1.6, the mechanism by which the Ras pathway is affected by the protein of interest, SHP2, is as follows.

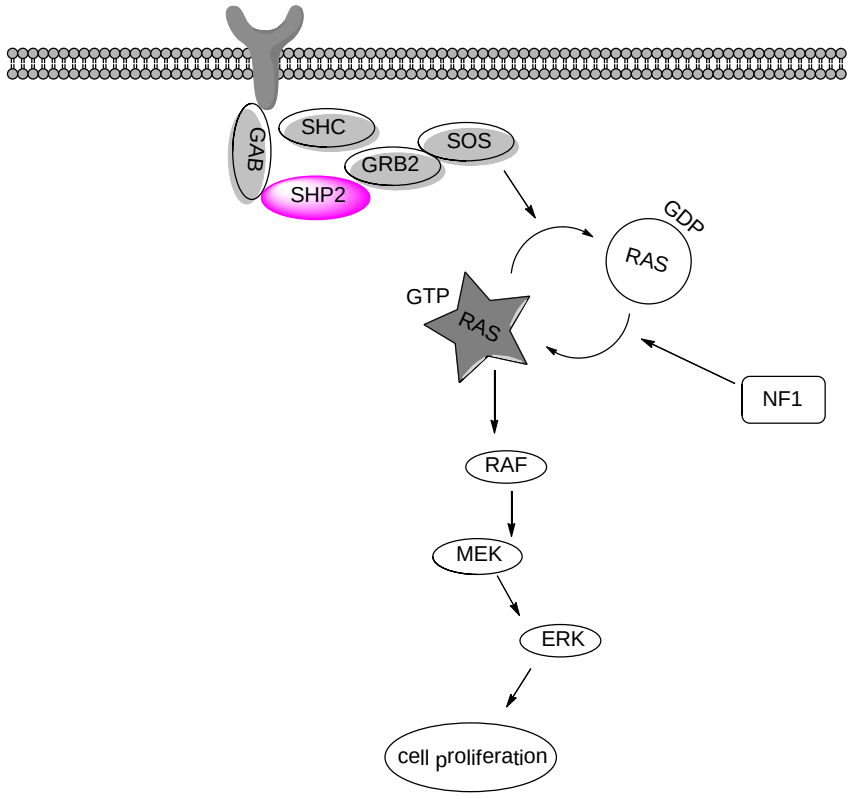

Figure 1.8 Simplified Ras Signal pathway in the cell.

The stimulating growth factor first binds to the receptor and causes the associated tyrosine kinases to phosphorylate tyrosine residues. These phosphorylated tyrosines then serve as binding sites for a series of adaptor proteins that activate the Ras protein and cause the binding of GTP and the release of GDP. The activated Ras triggers a cascade of phosphorylation reactions, starting with Raf. Raf phosphorylates MEK, a protein kinase, which then phosphorylates mitogen-activated protein kinases (MAPK). Activated MAPKs enter the nucleus and phophorylate regulatory transcription

factors, which activate transcription, and cause the cell cycle to move past the restriction point and into the S phase in the cell cycle.[29] (Figure 1.7) Upon inhibition of PTP-SHP2 activity in the Ras signaling pathway, Ras switches to a continuously 'on' state leading to the uncontrolled replication of cells, which is most commonly found in cancer cells.

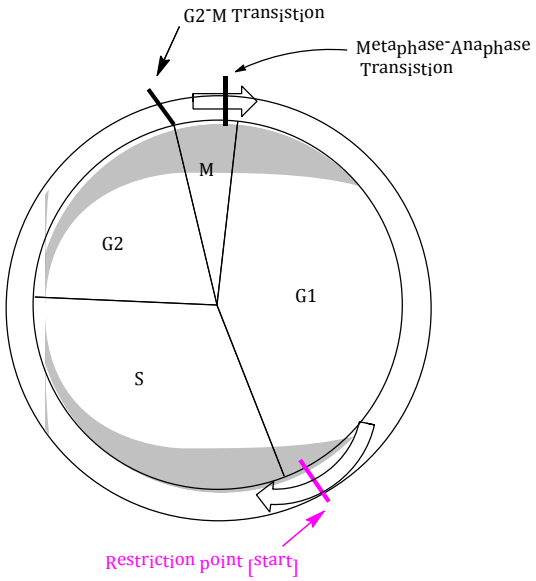

Figure 1.9 Simplified rendering of the cell cycle.[29]

The identity of SHP2s substrate remains the focus of current studies, and SHP2s role in the cell will help to determine the basis of its activity. Our group's research focuses on the identification of PTP family members and the regulation of these PTPs. The following chapters will focus on PTP-SHP2, its role within the cell, and the regulation of this PTP.

1.9 Goals of This Thesis

Due to their role in the control of important cellular signaling pathways, there is great interest in the development of selective inhibitors of PTPs. The focus of the Gate's research group has been to identify members of the PTP family and examine the regulation of these PTPs. The following chapters, I will focus on the regulation of PTP-SHP2 and its role within the cell.

In chapter 2, the inactivation of PTP-SHP2 by hydrogen peroxide and peroxy monocarbonate will be discussed. The kinetic inactivation of this PTP by the above agents will be presented, along with the recovery of activity.

Chapter 3 will cover the inactivation of PTP-SHP2 by dietary isothiocyantes. The inactivation and recovery of activity of SHP2 will also be presented.

1.10 References

(1) Hunter, T. *Cell* **2000**, *100*, 113.

(2) Chan, G.; Kalaitzidis, D.; Neel, B. *Cancer and Metastasis Reviews* **2008**, *27*, 179.

(3) Denu, J. M.; Tanner, K. G. *Biochemistry* **1998**, *37*, 5633.

(4) Galic, S.; Hauser, C.; Kahn, B. B.; Haj, F. G.; Neel, B. G.; Tonks, N. K.; Tiganis, T. *Mol. Cell. Biol.* **2005**, *25*, 819.

(5) Jiang, Z.-X.; Zhang, Z.-Y. *Cancer and Metastasis Reviews* **2008**, *27*, 263.

(6) Mohi, M. G.; Neel, B. G. *Current Opinion in Genetics & Development* **2007**, *17*, 23.

(7) NAIR, S.; LI, W.; KONG, A.-N. T. *Acta Pharmacologica Sinica* **2007**, *28*, 459.

(8) Stone, R. L.; Dixon, J. E. *Journal of Biological Chemistry* **1994**, *269*, 31323.

(9) Tonks, N. K. *Nature Reviews Molecular Cell Biology* **2006**, *7*, 833.

(10) Wang, S.; Yu, W.-M.; Zhang, W.; McCrae, K. R.; Neel, B. G.; Qu, C.-K. *Journal of Biological Chemistry* **2009**, *284*, 913.

(11) Andersen, J. N.; Mortensen, O. H.; Peters, G. H.; Drake, P. G.; Iversen, L. F.; Olsen, O. H.; Jansen, P. G.; Andersen, H. S.; Tonks, N. K.; Moller, N. P. H. *Mol. Cell. Biol.* **2001**, *21*, 7117.

(12) Salmeen, A.; Andersen, J. N.; Myers, M. P.; Meng, T.-C.; Hinks, J. A.; Tonks, N. K.; Barford, D. *Nature* **2003**, *423*, 769.

(13) Denu, J. M.; Lohse, D. L.; Vijayalakshmi, J.; Saper, M. A.; Dixon, J. E. *Proc Natl Acad Sci U S A* **1996**, *93*, 2493.

(14) Lohse, D. L.; Denu, J. M.; Santoro, N.; Dixon, J. E. *Biochemistry* **1997**, *36*, 4568.

(15) Winterbourn, C. C. *Nat Chem Biol* **2008**, *4*, 278.

(16) Stone, J. R. *Archives of Biochemistry and Biophysics* **2004**, *422*, 119.

(17) Goldstein, B. J.; Mahadev, K.; Wu, X. *Diabetes* **2005**, *54*, 311.

(18) Mahadev, K.; Motoshima, H.; Wu, X.; Ruddy, J. M.; Arnold, R. S.; Cheng, G.; Lambeth, J. D.; Goldstein, B. J. *Mol. Cell. Biol.* **2004**, *24*, 1844.

(19) Neel, B. P., Lily; Gu,Haihua In *Handbook of Cell Signaling Volume 1*; Bradsha, R. D., E., Ed.; Academic Press: San Diego, 2003; Vol. 1, p 707.

(20) Mahadev, K.; Zilbering, A.; Zhu, L.; Goldstein, B. J. *J Biol Chem* **2001**, *276*, 21938.

(21) van Montfort, R. L. M.; Congreve, M.; Tisi, D.; Carr, R.; Jhoti, H. *Nature* **2003**, *423*, 773.

(22) Claiborne, A. M., H.; Parsonage, D.; Ross, R.P. *FASEB Journal* **1993**, *7*, 1483.

(23) Neel, B. G.; Gu, H.; Pao, L. *Trends in Biochemical Sciences* **2003**, *28*, 284.

(24) Feng, G.-S. *Experimental Cell Research* **1999**, *253*, 47.

(25) Bentires-Alj, M.; Paez, J. G.; David, F. S.; Keilhack, H.; Halmos, B.; Naoki, K.; Maris, J. M.; Richardson, A.; Bardelli, A.; Sugarbaker, D. J.; Richards, W. G.; Du, J.; Girard, L.; Minna, J. D.; Loh, M. L.; Fisher, D. E.; Velculescu, V. E.; Vogelstein, B.; Meyerson, M.; Sellers, W. R.; Neel, B. G. *Cancer Research* **2004**, *64*, 8816.

(26) Huang, Q.; Lerner-Marmarosh, N.; Che, W.; Ohta, S.; Osawa, M.; Yoshizumi, M.; Glassman, M.; Yan, C.; Berk, B. C.; Abe, J. *J Biol Chem* **2002**, *277*, 29330.

(27) Le, L. Q. P., L.F. *Oncogene* **2007**, *25*, 4609.

(28) Shilyansky, C. L., Y.S.; Silva, A.J. *Annual review of Neuroscience* **2010**, *33*, 221.

(29) Becker, W. K., L.; Hardin, J. *The World Of The Cell*; 6th ed.; Pearson Education: San Francisco, 2006.

2.1 Introduction to Inactivation of Protein Tyrosine Phosphatase with H2O2.

A protein tyrosine phosphatse's (PTP's) activity can be modulated by the oxidation state of its catalytic cysteine (Cys215 in the prototypical numbering system of PTP1B).[1] The catalytic cysteine is especially prone to oxidation due to the lowered pK_a of 5.5.[2-5] This is roughly three pH units below a free cysteine.[6] Thus, the active site cysteine exists as a thiolate anion at physiological pH (pH=7) which is capable of nucleophilic attack on hydrogen peroxide (H_2O_2). As stated in Chapter 1, inactivation of PTP1 by H_2O_2[6] was ascertained to occur with a rate of 10-20 $M^{-1}s^{-1}$.[2,6-7] This rate constant has been reproduced for PTP1B by previous members of the Gates' group.[8-9]

It is known that members of the PTP family share a structurally homologous active site.[6,10] It is reasonable to assume that either all PTPs are able to undergo inactivation by H_2O_2, or this inactivation may be used further for selectivity. The rate of inactivation of PTPs may vary differently due to interactions of the active site with other structural features of each PTP, for example SHP2's *N*-SH2 domain. For this reason, investigating the inactivation of PTP-SHP2 by H_2O_2 was a priority in order to determine if oxidation of a PTP by H_2O_2 could be selective.

2.2 Kinetics of the Inactivation of PTP-SHP2 by Hydrogen Peroxide.

In this work, the kinetics of oxidation of SHP2 by H_2O_2 were explored in an effort to discover if H_2O_2 was able to selectively inactivate a PTP. Due to hydrogen peroxides ability to regulate the activity of PTP1B[6] with a second order rate constant of 10-20 $M^{-1}s^{-1}$,[2,6,8-9] it is important to see if this rate is comparable to that observed for the inactivation of SHP2 by H_2O_2.

To determine the rate of inactivation of SHP2 by H_2O_2, the enzyme (SHP2) was subjected to various concentrations of H_2O_2 and loss of enzymatic activity of SHP2 as a function of time was spectrographically monitored by release of *p*-nitrophenolate (Fig.2.1). Figure 2.1 illustrates how increasing concentrations of H_2O_2 yield increasing rates of SHP2 inactivation, which is analogous to observations made for PTP1B.

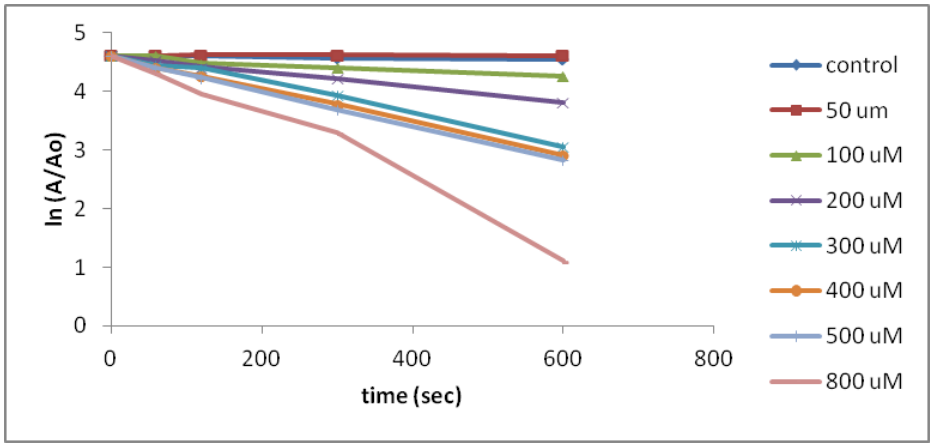

Figure 2. 1 Semilog plot of the inactivation of SHP2 with increasing concentrations of hydrogen peroxide [50 µM – 800 µM] n=6.

From the slopes of the lines in Figure 2.1, we were able to determine the pseudo-first-order rate constants for inactivation of SHP2 by H_2O_2 at various concentrations. By plotting the pseudo-first-order rates versus the concentrations of H_2O_2 the apparent second order rate of inactivation is obtained (Fig 2.2). The apparent second order rate of inactivation of SHP2 by H_2O_2 was found to be 14.2 ± 0.9 M^{-1} sec^{-1}. This observed rate constant is similar to those previously reported for inactivation of PTP1B by H_2O_2 (10-20 M^{-1} s^{-1}). [6,8-9]

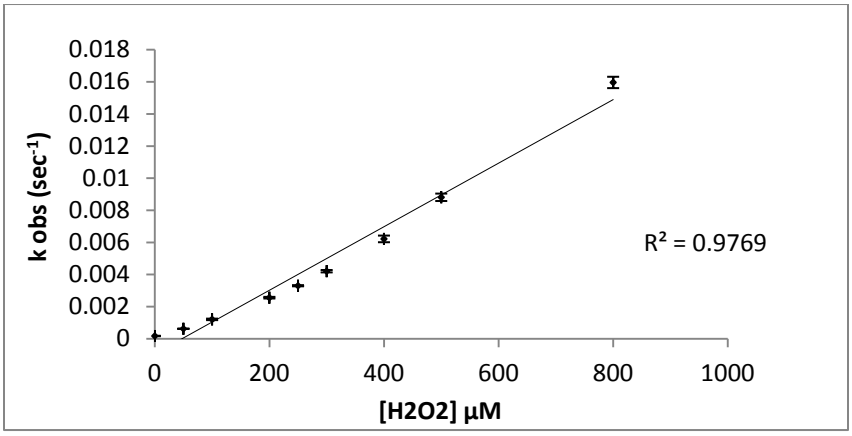

Figure2. 2 Inactivation of PTP-SHP2 by varying concentrations of hydrogen peroxide. The plot shows the pseudo-first-order rate constants versus the concentrations of hydrogen peroxide employed during the inactivation. Points represent the mean with standard error calculated, where n=6.

As stated previously, low micro molar concentrations of H_2O_2 have been shown to slowly inactivate PTP1B[6,8-9,11]. The rates used for inactivation *in vitro* indicate that inactivation within the cell, by H_2O_2 alone, would occur too slowly to explain the tight control observed with PTPs in cells. The comparable rate of inactivation of SHP2 by low micro-molar concentrations of H_2O_2 to PTP1B, shows that SHP2 exhibits the same rate of inactivation as PTP1B. Therefore the data presented here suggests that H_2O_2 is not

selective in inactivation of PTP1B versus SHP2 *in vitro*.

2.3 Introduction to the Formation of Peroxymonocarbonate.

The reaction between bicarbonate and H_2O_2 to form peroxymonocarbonate was observed using NMR by Flanagan and co-workers in 1986.[12] It was revealed that only a few species are formed during the reaction of bicarbonate with H_2O_2.[12] They were able to deduce that peroxymonocarbonate was formed via Reaction 2.1, upon addition of the bicarbonate to H_2O_2.[12-15]

$$HCO_3^- + H_2O_2 \rightleftharpoons HCO_4^- + H_2O$$ **Reaction 2.1**

The peroxymonocarbonate ion [HCO_4^-], which is the covalent adduct of peroxide anion [-OOH] and CO_2,[16] forms in water and buffered solutions at neutral pH (pH= 7.4) without the use of additional acids.[13,16] Researchers proposed the formation of peroxymonocarbonate in a biological system by the observed increase of methionine oxidation by H_2O_2 in the presence of bicarbonate.[17-19] Peroxymonocarbonate has been shown to be an activator for the oxidation of a nucleophile by H_2O_2.[13] This data, along with the knowledge that bicarbonate is present within cells at milli molar concentrations,(25 mM and 14.4 mM)[20] led to an increased interest in the role of peroxycarbonates in the oxidation of cysteine residues.

2.4 Kinetics of the Inactivation of PTP-SHP2 by Peroxymonocarbonate.

The addition of bicarbonate to H_2O_2 has been observed to increase the rate of inactivation of PTPs.[21-22] Thus investigating the oxidation of the catalytic cysteine by H_2O_2 in the presence of bicarbonate, it was revealed that peroxymonocarbonate is the relevant oxidant in the inactivation of PTPs. As previously described peroxymonocarbonate is formed when H_2O_2 reacts with bicarbonate[23] (see reaction 2.1).

In order to understand the mechanism which controls PTPs *in vivo*, identity of relevant ROS must be investigated. Therefore understanding how peroxymonocarbonate inactivates PTP is important. Inactivation of SHP2 by H_2O_2 + HCO_3^- was carried out. The first goal of this inactivation study was to observe if extracellular concentrations of bicarbonate (25 mM[20]) were capable of producing a rate of inactivation on the same order of magnitude as seen in a signaling cascade[21].

Figure 2.3 illustrates that increasing concentrations of H_2O_2 in the presence of 25 mM bicarbonate increased the rate of inactivation of the enzyme versus inactivation by H_2O_2 alone. Using the slopes from Figure 2.3 the pseudo-first-order-rates of inactivation at various H_2O_2 concentrations were found and these rates were plotted versus [H_2O_2] to determine the apparent second order rate constant for inactivation by H_2O_2/HCO_3^-.

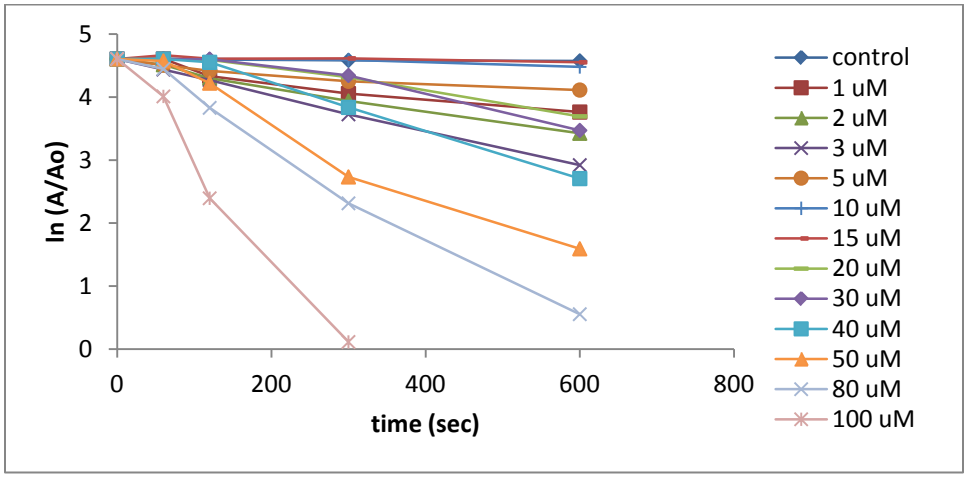

Figure 2.3 Semilog plot of the inactivation of SHP2 with 25 mM $KHCO_3$ and increasing concentrations of hydrogen peroxide [1 µM - 15 µM] where n=6.

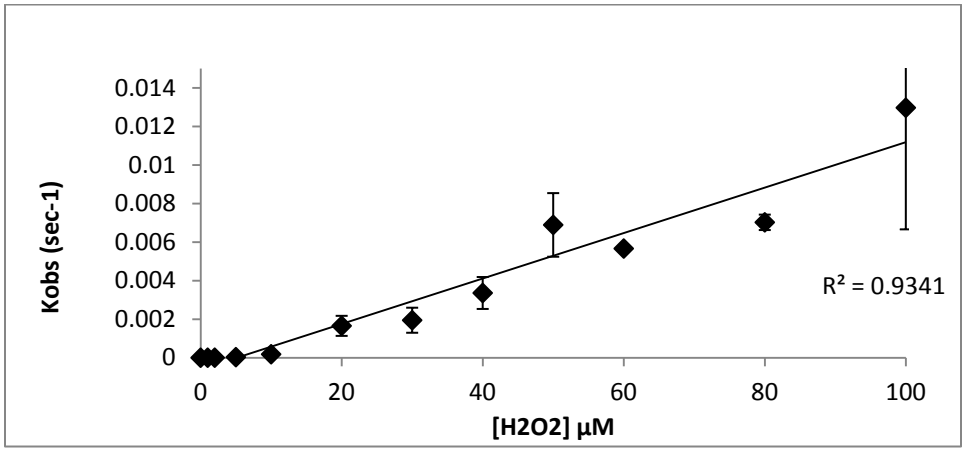

Figure 2.4 Inactivation of PTP-SHP2 with 25 mM $KHCO_3$ with various concentrations of hydrogen peroxide [1 µM - 15 µM] yields a second order rate constant. Points represent the mean with standard error calculated where n=6.

The apparent second order rate of inactivation by H_2O_2 for SHP2 in the presence of 25 mM bicarbonate was found to be 117.88 $M^{-1}s^{-1}$ (Figure 2.4).We observed a 10 fold increase when comparing the rate of inactivation of SHP2 by H_2O_2 alone, 14.28 $M^{-1}s^{-1}$, to the apparent second order rate of inactivation by H_2O_2 and potassium bicarbonate.

When utilizing intracellular concentrations of bicarbonate [14.4 mM],[20] a slightly lower rate of inactivation is observed compared to that observed for 25 mM bicarbonate. Figure 2.5 illustrates the decreasing activity of SHP2 as the concentration of H_2O_2 [20 µM – 100 µM] increases.

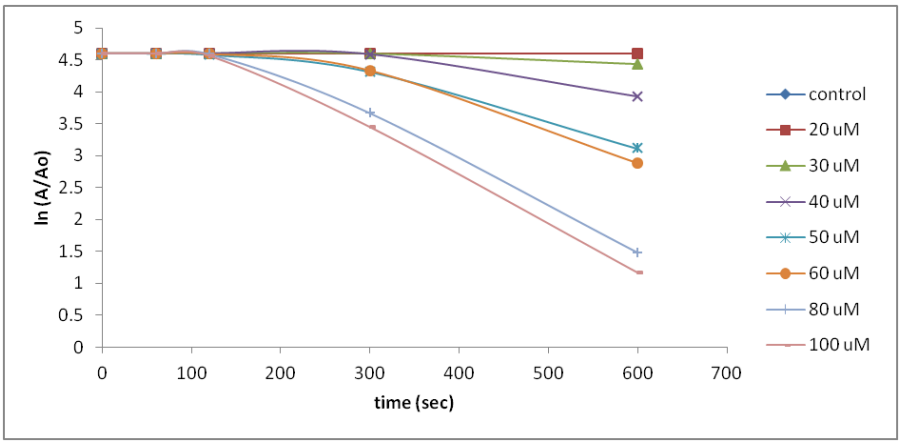

Figure 2.5 Semilog plot of the inactivation of SHP2 in the presence of 14.4 mM $KHCO_3$ and various concentrations of hydrogen peroxide [20 µ M - 100 µM] where n=6.

The apparent second order rate of inactivation in the presence of 14.4 mM bicarbonate was determined to be 75.21 $M^{-1}s^{-1}$ (Figure 2.6). This was obtained from the pseudo-first-order inactivation rates (taken from the slopes of figure 2.5).These pseudo-first-order rates were re-plotted versus the concentrations of H_2O_2 added during the assay to give the apparent second order rate of inactivation of SHP2.

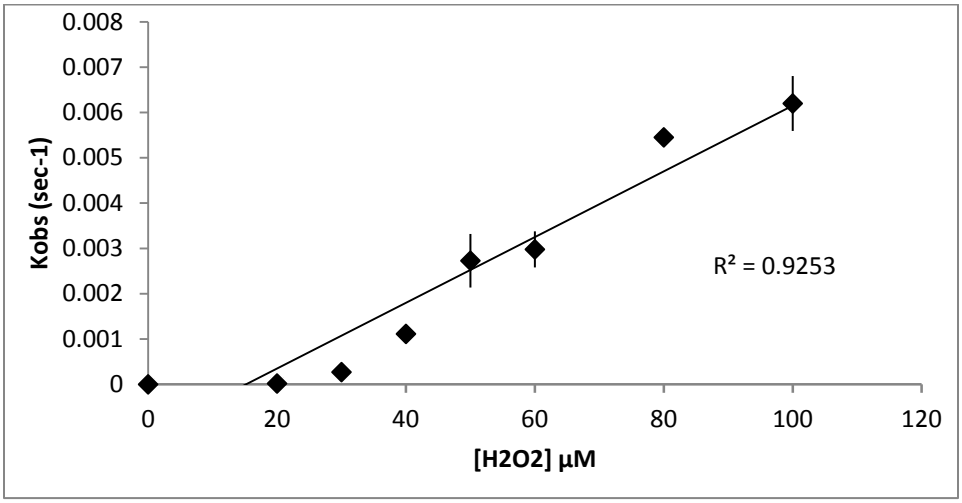

Figure 2.6 Inactivation of PTP-SHP2 by hydrogen peroxide with 14.4 mM $KHCO_3$. The apparent second order rate constant was calculated with each point being the mean with standard error where n=6.

The rate of inactivation of PTP1B by peroxymonocarbonate was identified to be 202 ± 4 M^{-1} s^{-1}.[24] This rate is on the same order of magnitude as that seen by SHP2 and thus supports the hypothesis that the presence of bicarbonate within the cell does effect the oxidation of the catalytic cysteine (SHP2-Cys459). The presence of bicarbonate also allow for the inactivation of PTPs by H_2O_2 at the low micro-molar concentrations observed in the cell[2] within the expected time frame of 10-15 minutes. However this time frame is not comparable to those during PTP regulation and thus it is assumed that the formation of peroxymonocarbonate works along with other systems to generate ROS within the cell.

2.5 Effect of Increased Bicarbonate Concentrations on the Inactivation of PTP-SHP2.

To examine the effect of HCO_3^- concentration on H_2O_2 mediated inactivation of PTPs, SHP2 was inactivated in the presence of micro-molar concentrations of H_2O_2 with increasing concentrations of potassium carbonate (Figure 2.7).

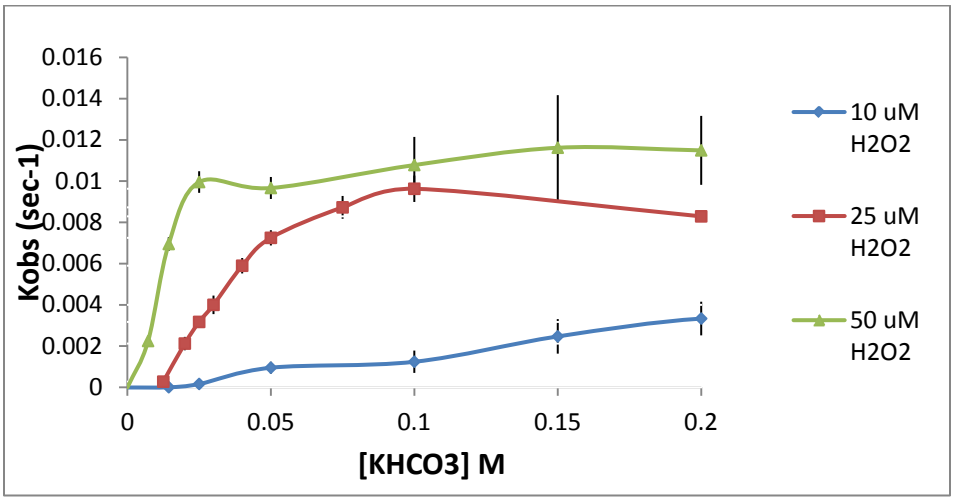

Figure 2.7 Inactivation of SHP2 with increasing concentrations of potassium carbonate and micro-molar concentrations of hydrogen peroxide. Points represent calculated mean with standard error shown, where n=6.

As shown in Figure 2.7 at higher concentrations of bicarbonate in H2O2, [50 µM], inactivation of SHP2 appears to plateau. This plateau effect could be attributed to saturation kinetics, meaning the enzyme experiences a loading up of inactivator to the active site. A probable explanation would be if HCO_3^- is sequestered to the active site where it can bind with H_2O_2 to form a more reactive oxidant, peroxymonocarbonate (Scheme 2.1).

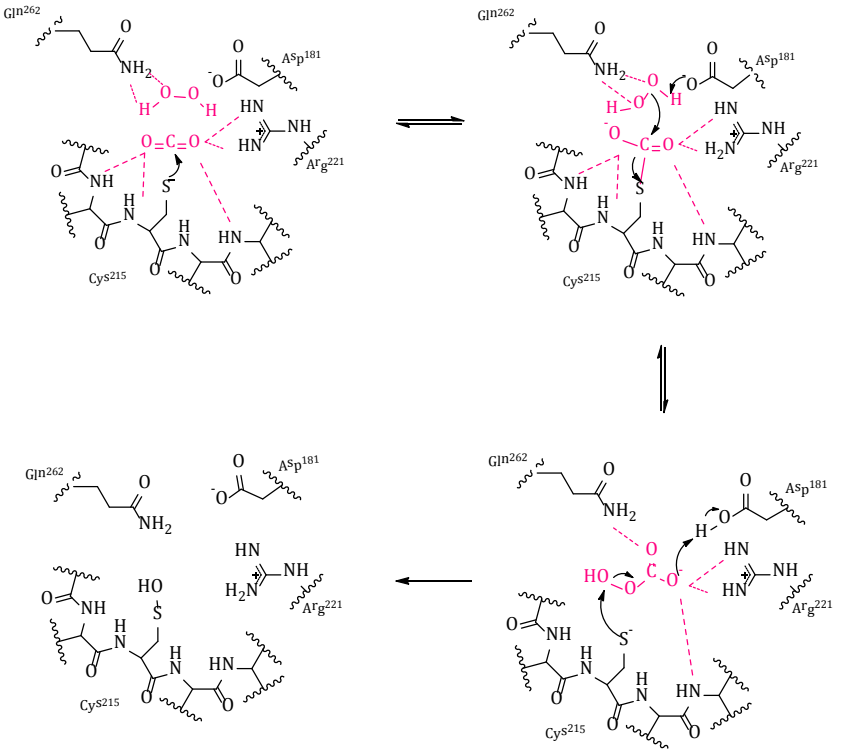

Scheme 2.1 Proposed mechanism for the formation of peroxymonocarbonate upon the active site of PTP1B

With this reaction taking place at the active site, it would explain how bicarbonate alone cannot inactivate PTPs, also how incubation of H_2O_2 and bicarbonate before inactivation of PTP does not seem to have an effect on the rate of inactivation. Further investigation into the stability of bicarbonate during assay conditions employed is necessary to aid in the verification of this theory.

2.6 Bicarbonate Stability.

Inactivation studies of PTP1B and SHP2 with potassium bicarbonate in the presence of H_2O_2 revealed a plateau or saturation effect, at higher concentrations of bicarbonate [100 mM – 300 mM]. The formation of peroximonocarbonate at the active site of PTPs was suggested to aid in the explanation of the data obtained, however, the stability of the bicarbonate solutions needed to be ascertained under regular assay conditions.

The specific investigation of loss of HCO_3^-/CO_2 from concentrated solutions of $KHCO_3$ over time was carried out by determination of the concentration of bicarbonate during an assay. Since barium carbonate ($BaCO_3$) is insoluble in water,[25] a protocol was developed to assess the concentration of bicarbonate in a typical assay. Approximately 10% w/v of $BaCl_2$ was added to various concentrations of potassium bicarbonate solution [100 mM – 300 mM] to the buffer system utilized in previous inactivation studies (50 mM Bis-Tris, 50 mM Tris, 10 mM DTPA, and 100 mM NaOAc at pH 7.0). In an attempt to replicate the assay conditions 10 mL solutions of buffer were incubated as previously described. After incubation, $BaCl_2$ was added and the resulting precipitate (Reaction 2.2) was collected by centrifugation (2000 rpms for 30 minutes) dried overnight, and weighed.

$$BaCl_2\,(s) + CO_3^{2-}\,(aq) \longrightarrow BaCO_3\,(s)\downarrow + 2Cl^{2-}\,(aq)$$ **Reaction 2.2**

Confirmation that resulting solid was $BaCO_3$ was confirmed by flame test. The precipitate was placed in a flame and the resulting green color, which is indicative of the presence of barium, was recorded[26]. This test was utilized only as a method of qualitative analysis, given that; this test shows the presence of barium but does not exclude the presence of other molecules. It was determined that the amount of $BaCO_3$ precipitated was directly proportional to the expected $KHCO_3$ in solution. Thus providing evidence that inactivation of PTP was occurring with the concentrations previously assumed (Table 2.1), and there is no significant loss of HCO_3^- during the assays.

	Trial 1				Trial 2				Trial 3			
$BaCO_3$ (grams)												
[$KHCO_3$]	**0 mM**	**100 mM**	**200 mM**	**300 mM**	**0 mM**	**100 mM**	**200 mM**	**300 mM**	**0 mM**	**100 mM**	**200 mM**	**300 mM**
20 mins 'hot'	0	0.1734	0.3391	0.3578	0	0.162	0.334	0.3175	0	0.1619	0.3691	0.3701
20 mins open	0	0.1655	0.384	0.6056	0	0.1799	0.3582	0.315	0	0.1646	0.3478	0.374
150 mins open	0	0.1742	0.3678	0.3323	0	0.1635	0.3654	0.3155	0	0.1595	0.3756	0.3603
$BaCO_3$ (moles)												
[$KHCO_3$]	**0 mM**	**100 mM**	**200 mM**	**300 mM**	**0 mM**	**100 mM**	**200 mM**	**300 mM**	**0 mM**	**100 mM**	**200 mM**	**300 mM**
20 mins 'hot'	0	0.00088	0.00172	0.00181	0	0.00082	0.00169	0.00161	0	0.00082	0.00187	0.00188
20 mins open	0	0.00084	0.00195	0.00307	0	0.00091	0.00182	0.0016	0	0.00083	0.00176	0.0019
150 mins open	0	0.00088	0.00186	0.00168	0	0.00083	0.00185	0.0016	0	0.00081	0.0019	0.00183

Table 2.1 Recovery of Barium carbonate from assay of the concentration of potassium carbonate in peroxymonocarbonate inactivation of PTPs.

In order to determine if there was a significant change in the pH during a typical assay, the pH at higher concentrations of bicarbonate [100 mM – 300 mM] was quantified. An increase in the concentration of potassium carbonate within the buffer system can affect the pH of the system under investigation. The pK_a of the carbonic acid is 6.4,[25]. This would increase the concentration of applicable H^+ allowing for increased formation of the cysteine thiol. Since the thiolate ion is the active form of the catalytic

cysteine in PTPs, this would result in invalid data. It was observed that higher concentrations of bicarbonate do raise the pH of the system during an assay and thus have the potential to affect the activity of the catalytic cysteine (see Table 2.2 and Figure 2.8).

[$KHCO_3$]		**0 mM**	**25 mM**	**50 mM**	**100 mM**	**200 mM**	**300 mM**
pH	**trial 1**	7.00	7.06	7.19	7.37	7.57	7.72
	trial 2	6.99	7.08	7.17	7.29	7.46	7.56
	trial 3	6.97	7.09	7.18	7.39	7.57	7.70
	trial 4	6.94	7.07	7.20	7.39	7.56	7.69

Table 2.2 Effect of high concentrations of $KHCO_3$ on the pH of assay buffered solutions

In Figure 2.8 it is observed that concentrations of bicarbonate from 150 mM to 300 mM causes such a pH effect that the pseudo first order rate of inactivation of these values does not follow the trend of the previous data points. If the apparent second order rate of inactivation is determined from these flawed data, we calculate that rate to be 0.0168 $M^{-1}s^{-1}$ (Figure 2.8).

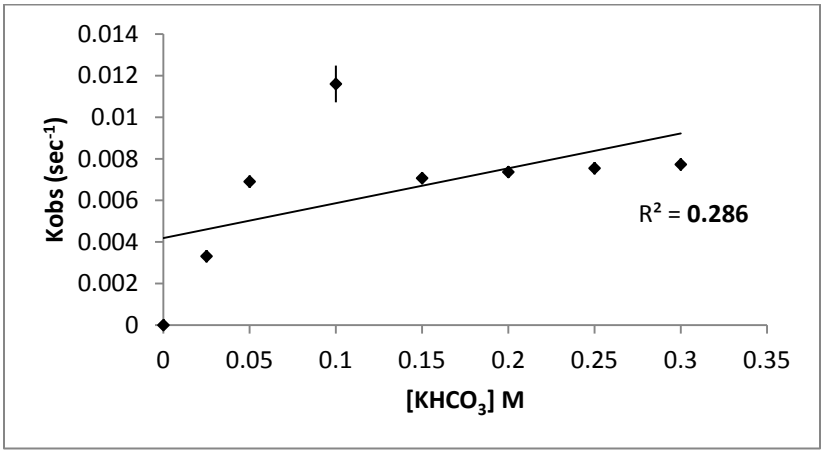

Figure 2.8 Inactivation of PTP1B in normal assay buffer system. A calculated second order rate of inactivation was determined to be 0.0168 M^{-1} s^{-1} where the mean is shown with standard error calculated and n=4.

In order to ensure that the previously obtained rate of inactivation was still applicable, the pH was controlled at the higher concentrations of bicarbonate by changing the buffer system (300 mM Tris, 300 mM Bis-Tris, 60 mM DTPA, and 600 mM NaOAc). The apparent second order rate of inactivation was determined to be 0.0233 $M^{-1}s^{-1}$ (Figure 2.9) which is analogous to the results found for the inactivation of PTP1B with high concentrations of bicarbonate (Figure 2.9) in the original buffer system.

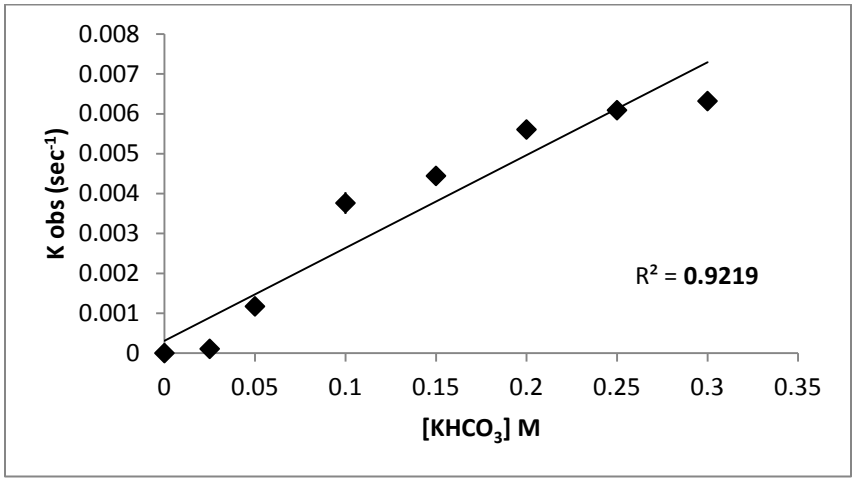

Figure 2. 9 Inactivation of PTP1B with increased concentrations of Tris and Bis-Tris to control the pH at high concentrations of bicarbonate. An apparent second order rate of inactivation was determined to be 0.0233 $M^{-1}s^{-1}$. The data points shown represent the mean with standard error calculated where n=4

This "beefed up" version of the normal three component assay buffer was used to ensure that the concentration of Tris and Bis-Tris were the same as the highest concentration of potassium bicarbonate, thus confirming that the catalytic cysteine is in the active thiolate form at high concentrations of bicarbonate. Further inactivation by peroxymonocarbonate was carried out in the original buffer system taking into consideration that the rate of inactivation would only hold true when lower concentrations of potassium bicarbonate were present.

2.7 Discussion.

We have provided evidence that H_2O_2 is not a plausible selective inhibitor of PTPs. The apparent second order rate of inactivation of SHP2 was found to be 14.2 ± 0.9 M^{-1} s^{-1}which is the same order of magnitude as the reported value of PTP1B (10-20 M^{-1} s^{-1}).[6,8-9] We have also concluded that inactivation of SHP2 by peroxymoncarbonate (117.88 $M^{-1}s^{-1}$) is analogous to the values observed for PTP1B (202 ± 4 M^{-1} s^{-1}) (Zhou,H. unpublished data).

Confirmation of concentrations of peroxmonocarbonate were carried out and it was determined that the bicarbonate is stable in the buffer system used. Although the pH is affected by the addition of high concentrations of bicarbonate (100-300 mM) to the system, the rate of inactivation obtained at these values is applicable.

2.8 Materials and Methods

2.8.1 Chemicals and Reagents

Reagents were purchased from the following suppliers: Buffer salts, *p*-nitrophenylphosphate (pNPP), thiols, ampicillin, chloramphenical, Luria Broth Media, Isopropylβ-D-1-thiogalactopyranoside, DL-Dithiothreitol, Diethylenetriaminepentaacetic acid (DTPA), Deoxyribobuclease I bovine, Kanamycin disulfide salt, Imidazole, HEPES, and Sodium Acetate (99+%) were obtained from Sigma-Aldrich (St.Louis MO). Zeba mini and micro centrifugal buffer exchange columns (catalog number 89882) and Surfact-Amps 80 (Tween), 10% solution, catalog number 28328) were obtained from Pierce Biotechnology (Rockford,IL). Restriction endonucleases EcoRI (catalog number R0101) and SmaI (catalog number R0141) were obtained from New England Biolabs [Ipswich, MA). BL21 DE3 compotent cells (catalog number 11665-015) were obtained from Invitrogen (Carlsbad, CA). Overnight Express Autoinduction System 1 Kit (catalog number 71300-4) was purchased from Novagen (Madison, WI). Sodium Chloride (catalog number S271), hydrogen peroxide (30%) (catalog number H325) and Potassium Bicarbonate (catalog number P184) were purchased from Fisher Chemical [Fair Lawn, NJ).

2.8.2 Recombinant Expression of PTP-SHP2

DNA coding for the His-tagged catalytic subunit of SHP2 was amplified from plasmid obtained from Structural Genomics Center. The resulting construct was purified using a 0.8% agarose gel. The plasmid was isolated with Promeaga Wizard Plus Plasmid DNA columns

Escherichia coli DH5α cells were transformed according to protocol with purified plasmids from amino acids 246-527 containing 36 kDa SHP2. Plasmid DNA from these DH5α cells was extracted and transformed into BL21 DE3 cells according to the manufacturer's protocol. Cells were selected on LB agar with kanamycin (30 μg/mL), a monoclonal sample from was placed into 0.5 L cultures of Luria Broth Kanamycin (30 μg/mL), and autoinduction media from Novagen's Overnight Express Autoinduction System 1 kit and grown for 22 hours at 18°C with 250 rpms until stationary phase was reached (which was determined by $A_{600} \geq 0.8$). Cells were harvested by centrifugation at 5000 x *g* for 30 minutes; the cell pellet was resuspended in 50 mL of binding buffer (50mM HEPES pH 7.0, 500mM NaCl, 5mM imidazole, and 0.5mM TCEP). The cells were then lysed by French Press in the presence of DNase (Deoxyribonuclease I bovine). The resulting lysate was centrifuged for 30 minutes at 3700 x *g*. After removal of DNA fragments (unbroken cells and debris) the resulting supernant was loaded onto a 5mL HisTrapHP column and equilibrated with additional lysis buffer. SHP2 was eluted with a 0 to 1 M linear gradient of imidazole at a rate of 2 mL/min. Two mL fractions were collected with an AKTAprime fraction collector system. These fractions were tested for

activity with *p*-nitro phenyl phosphate (*p*NPP) and pooled. The pooled fractions were dialyzed into a 50 mM Tris buffer with 0.5 M NaCl, then loaded onto a 1.0 mL Q-sepharose column and eluted with a 25 mL gradient from 0 to 1 M NaCl linear gradient. Collected fractions were again tested for activity with *p*NPP, pooled and concentrated to 0.5 mg/mL total protein. Protein concentration was determined by the utilization of Beer's Law (equation 2.1):

$$A = \varepsilon bc \qquad \textbf{Equation 2.1}$$

The concentration is multiplied by the weight of SHP2 DNA (36823.59 g/mol). Once concentration was determined the resulting pool is divided into 100 µL aliquots and stored at -80°C until further use.

2.8.3 Time-Dependent Inactivation of PTP-SHP2

Inactivation kinetic assays were performed using existing group protocols.[9] Modifications of existing literature protocols[27-28] were made. Free thiols were removed from stock solutions of purified PTP-SHP2 using Zeba mini centrifugal exchange columns according to the manufacturer's protocol. The exchange buffer contained 50 mM Bis-Tris, 50 mM Tris, 1.0 mM DTPA, 100 mM NaOAc, and Tween 80 [0.05%] at pH 7.0. During the inactivation reactions, inactivators (hydrogen peroxide or hydrogen peroxide + potassium bicarbonate) were added as varying concentrations of inactivator in exchange buffer to SHP2 at 30°C, (final concentration of SHP2 ~20 nmol) final volume

was 100 µL. A 10 µL aliquot was removed at various time points (1 minute, 2 minutes, 5 minutes, and 10 minutes) and placed into 490 µL of assay buffer (50 mM Bis-Tris, 100 mM NaCl, 10 mM DTPA, and 20 mM pNpp pH 6.0) at 37°C for 10 additional minutes. The enzymatic reaction was quenched with the addition of NaOH (500 µL of 2 M solution in water). The amount of p-nitrolphenolate released during the reaction was determined by UV-vis measurement of the absorbance at 25°C and 405 nm.

2.9 References

(1) Hunter, T. *Cell* **2000**, *100*, 113.

(2) Tonks, N. K. *Nature Reviews Molecular Cell Biology* **2006**, *7*, 833.

(3) Chan, G.; Kalaitzidis, D.; Neel, B. *Cancer and Metastasis Reviews* **2008**, *27*, 179.

(4) van Montfort, R. L. M.; Congreve, M.; Tisi, D.; Carr, R.; Jhoti, H. *Nature* **2003**, *423*, 773.

(5) Salmeen, A.; Andersen, J. N.; Myers, M. P.; Meng, T.-C.; Hinks, J. A.; Tonks, N. K.; Barford, D. *Nature* **2003**, *423*, 769.

(6) Denu, J. M.; Tanner, K. G. *Biochemistry* **1998**, *37*, 5633.

(7) Chen, C.-Y.; Willard, D.; Rudolph, J. *Biochemistry* **2009**, *48*, 1399.

(8) LaButti, J. N., University of Missouri, 2009.

(9) Seiner, D. R., Missouri, 2009.

(10) Andersen, J. N.; Mortensen, O. H.; Peters, G. H.; Drake, P. G.; Iversen, L. F.; Olsen, O. H.; Jansen, P. G.; Andersen, H. S.; Tonks, N. K.; Moller, N. P. H. *Mol. Cell. Biol.* **2001**, *21*, 7117.

(11) LaButti, J. N.; Chowdhury, G.; Reilly, T. J.; Gates, K. S. *J Am Chem Soc* **2007**, *129*, 5320.

(12) Flangan, J.; Jones, D. P.; Griffith, W. P.; Skapski, A. C.; West, A. P. *Journal of the Chemical Society, Chemical Communications* **1986**, 20.

(13) Richardson, D. E.; Yao, H.; Frank, K. M.; Bennett, D. A. *Journal of the American Chemical Society* **2000**, *122*, 1729.

(14) Sharma, M. M.; Danckwerts, P. V. *Transactions of the Faraday Society* **1963**, *59*, 386.

(15) Palmer, D. A.; Van Eldik, R. *Chemical Reviews* **1983**, *83*, 651.

(16) Bakhmutova-Albert, E. V.; Yao, H.; Denevan, D. E.; Richardson, D. E. *Inorganic Chemistry* **2010**, *49*, 11287.

(17) Sankarapandi, S.; Zweier, J. L. *Journal of Biological Chemistry* **1999**, *274*, 1226.

(18) Trindade, D. F.; Cerchiaro, G.; Augusto, O. *Chemical Research in Toxicology* **2006**, *19*, 1475.

(19) Liochev, S. I.; Fridovich, I. *Free Radical Biology and Medicine* **2010**, *48*, 1565.

(20) Medinas, D. B.; Cerchiaro, G.; Trindade, D. F.; Augusto, O. *IUBMB Life* **2007**, *59*, 255.

(21) Winterbourn, C. C. *Nat Chem Biol* **2008**, *4*, 278.

(22) Stone, J. R. *Archives of Biochemistry and Biophysics* **2004**, *422*, 119.

(23) Flanagan, J. J., P.; Griffith, W.; Skaspski,A; and West, A *J.Chem.Soc., Chem. Commun.* **1986**.

(24) Zhou, H.; Singh, H.; Parsons, Z. D.; Lewis, S. M.; Bhattacharya, S.; Seiner, D. R.; LaButti, J. N.; Reilly, T. J.; Tanner, J. J.; Gates, K. S. *Journal of the American Chemical Society* **2011**, *133*, 15803.

(25) Harris, D. C. *Quantitative chemical analysis*; 6th ed.; W.H. Freeman and Co.: New York, 2003.

(26) Petrucci, R. H. *General chemistry : principles and modern applications*; 9th ed.; Pearson/Prentice Hall: Upper Saddle River, N.J., 2007.

(27) Silverman, R. B. In *Methods in Enzymology*; Daniel, L. P., Ed.; Academic Press: 1995; Vol. Volume 249, p 240.

(28) Montalibet, J.; Skorey, K. I.; Kennedy, B. P. *Methods* **2005**, *35*, 2.

3.1 Introduction to Isothiocyanates.

Isothiocyanates such as allyl isothiocyanate and sulforaphane (Scheme 3.1) are derived from glucosinolates, a group of dietary compounds that are found in *Brassica* vegetables. Examples of the *Brassica* family include broccoli, cabbages, sprouts, kale, turnips, watercress, and mustard seeds[1-12]. These cruciferous vegetables contain glucosinolates[3] which upon cellular break down release isothiocyanates by hydrolysis[12], which will be further discussed in more detail.

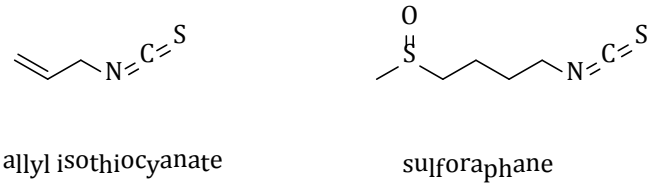

allyl isothiocyanate sulforaphane

Scheme 3.1 Examples of dietary isothiocyanates found in cruciferous vegetables

Isothiocyanates are formed and stored in plants as the stable precursors glucoraphanin and sinigrin.[2,4-5,13,10] These precursors are hydrolyzed to isothiocyanates by the plant enzyme myrosinase upon destruction of the plants via cutting or chewing.[1-5,13-15] Broccoli predominately contains the glucosinolate, glucoraphanin[4], which upon

hydrolysis forms sulforaphane (Scheme 3.2). Most other cruciferous vegetables contain sinigrin which can react to form a variety of isothiocyanates.[2,5,15] The research presented here focuses on allyl isothiocyanate (Scheme 3.3). Allyl isothiocyanate is believed to contribute to the distinctive flavor of some cruciferous foods[3] as well as the 'bite' of mustard.[3,16]

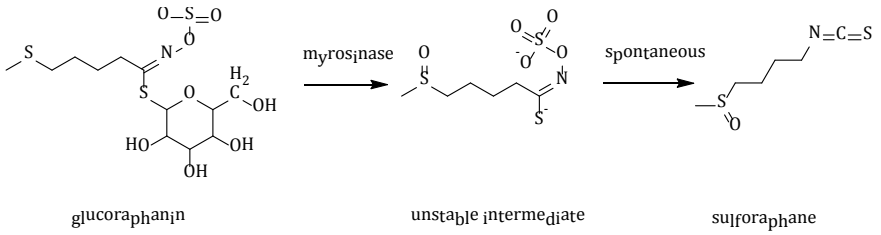

Scheme 3.2 Glucoraphanin is converted to sulforaphane through enzymatic hydrolysis by myrosinase.

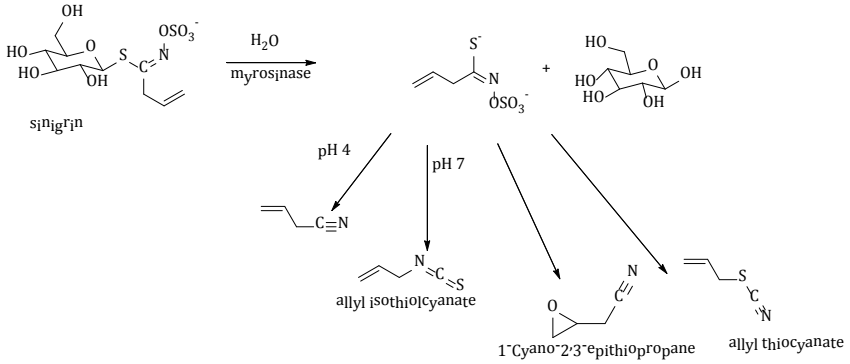

Scheme 3.3 Sinigrin is hydroylzed by myrosinase to yeild allyl isothiocyanate at neutral pH.

In the United States it is estimated that the average glucosinolate consumption is 0.6 µmol/day,[4] where as in other nations the daily consumption is larger. This value is estimated to be lower in western countries because most cruciferous vegetables

consumed are cooked,[4] accounting for the loss of nearly 30% of glucosinolates.[4] Myrosinase activity is inhibited during cooking so the conversion of glucosinolates to isothiocyanates relies on intestinal degradation.[4,9]

3.2 Isothiocyanate Activity Within the Cell.

Isothiocyanates have been shown to induce phase 2 enzymes,[6,17-18] cause cell death[11], and cause cell cycle arrest in the G_2/M phase.[6] Interestingly, isothiocyanates have been shown to act as electrophiles that are subject to nucleophilic attack by cysteine residues in biologically critical proteins (Scheme 3.4).[11,19]

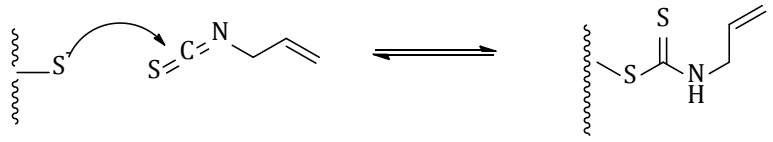

Scheme 3. 4 Thiolate from critical cysteine residue attacks the electrophilic isothiocyanate

Sulforaphane has been discovered as a cancer blocking agent via induction of phase 2 enzymes[8-9,11-12,18-21] and as a suppressing agent by inhibiting the progression of cancer cells through cell cycle arrest.[7,9,11,19,22] Induction of phase 2 enzymes have been correlated to the ability of sulforaphane to covalently modify a critical cysteine residue (Cys151) in Kelch-like ECH-associated protein 1 (Keap1).[9,23] This modification of Keap1 causes structural changes that release nuclear factor-erthroid-2-related factor 2 (Nrf2)[23]. Upon release, Nrf2 translocates to the nucleus and binds to either antioxidant response

elements (ARE) or electrophile response elements (EpRE) that encode for antioxidant/detoxifying enzymes[21](Scheme 3.5). Sulforaphane has also been shown to alter activity of cytochrome P450 (CYP) isoforms through a competitive mechanism, as well as by covalent modification[11]. The inhibition of CYP isoforms inhibits formation of DNA adducts by procarcinogens that are converted to carcinogens by P450s, unscheduled DNA synthesis, and CYP mediated DNA strand breakage.[11,24-25]

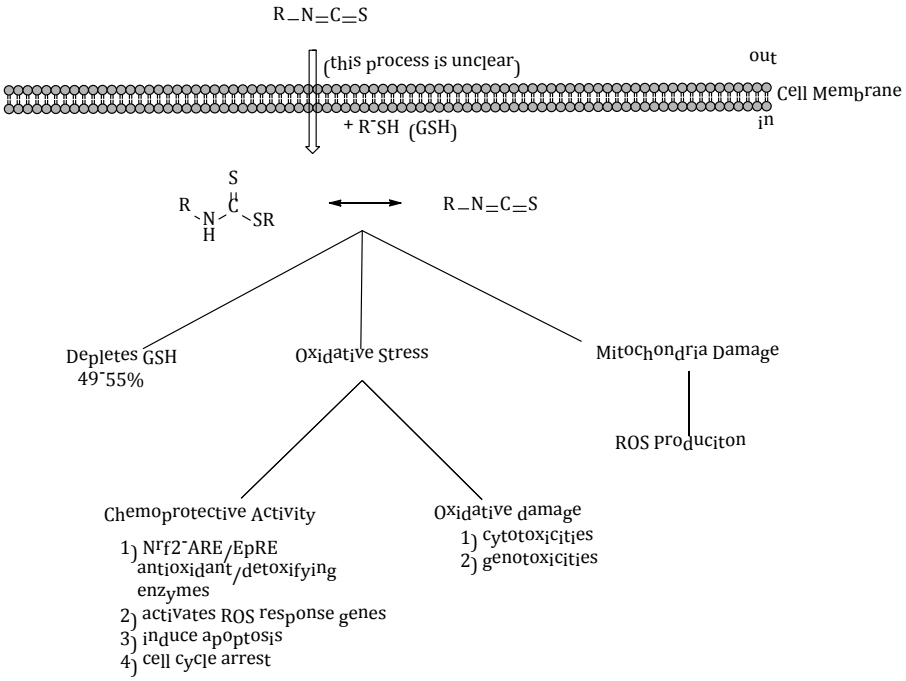

Scheme 3.5 Brief visualization of ITCs effects in the cell.[9,26]

Although among the ITCs sulforaphane has received the most attention, other isothiocyanates also exhibit potent biological activities. Allyl isothiocyanate which is most commonly found in cruciferous vegetables other than broccoli[1-5] such as mustard seeds, cabbage, and cauliflower, has significant biological activity.[1,3-4,6] Similar to

sulforaphane, allyl isothiocyanate can induce phase 2 enzymes in mice.[1,4] Allyl isothiocyanate is also able to cause apoptosis in prostate cancer cells by cell cycle arrest in the G2/M phase.[1,3,6] Xiao and coworkers[1], determined that apoptosis could be induced by allyl isothiocyanates due to its effect on capase-3, a cysteine-aspartic acid protease, activity on human prostate cancer cells. It was determined that caspase-3 like activity rose in cells treated with allyl isothiocyanates.[1] These results were confirmed by other groups studying the effects of allyl isothiocyanate treatment on cancerous cell lines as well.[6,27]

3.3 Kinetics of Inactivation of PTP-SHP2 by Isothiocyanates

Due to the increased attention given to isothiocyanates (ITCs), it is important to discern their mechanism of action within cells. Here, we tested the ability of sulforaphane and allyl isothiocyanate (AITC) to inactivate SHP2, a protein tyrosine phosphatase (PTP). Inactivation of SHP2 within the cell could account for the ability of ITCs to cause cell cycle arrest in the G2/M phase. Indeed, previous work has shown that inactivation of SHP2 in the Ras signaling pathway can lead to cell cycle arrest.[28-29]

It was determined that ITCs are time- and concentration-dependent inactivators of SHP2. This inactivation was initially investigated with the most common ITC in cruciferous vegetables, allyl isothiocyanate (AITC), (Figure 3.1)

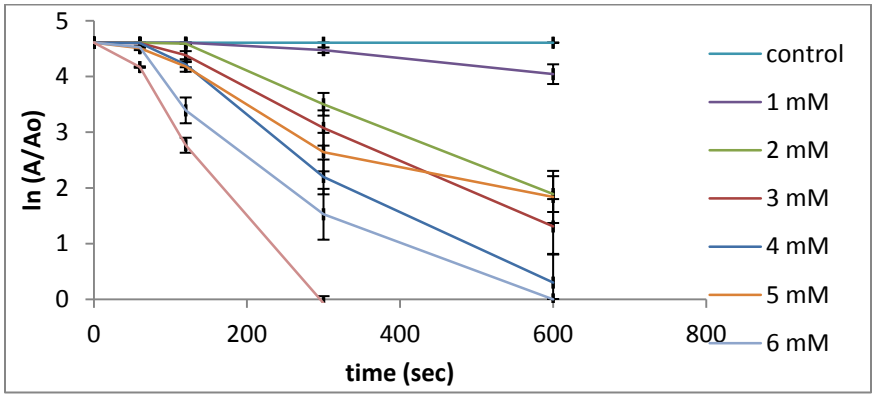

Figure 3.1 Natural log of percent inactivation of SHP2 with concentrations of ally isothiocyanate where n=6

The pseudo-first-order rates of inactivation of SHP2 were calculated using concentrations of AITC shown in Figure 3.1. These pseudo-first-order rates were re-plotted against the concentrations of AITC and the apparent second order rate of inactivation was calculated to be 2.0 ± 0.1 M^{-1} s^{-1} (Figure 3.2).

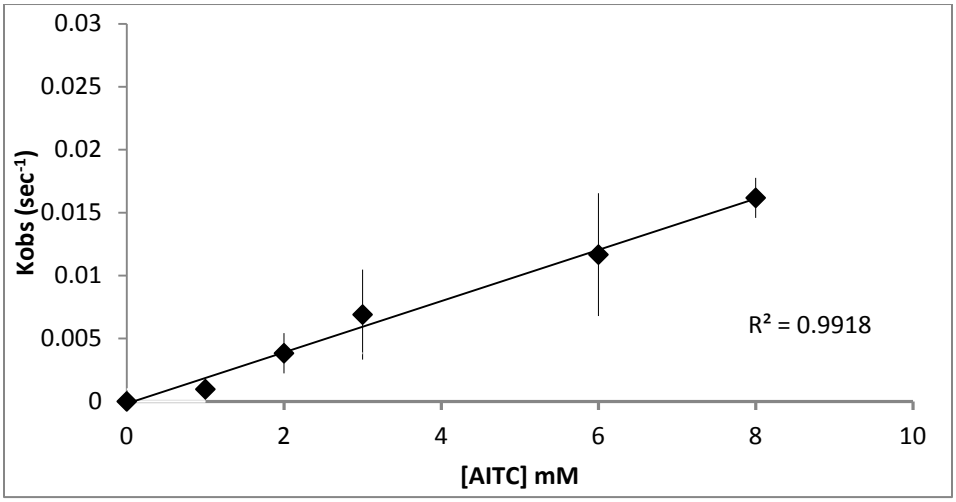

Figure 3.2 Inactivation of PTP-SHP2 with allyl isothiocyanate gives the apparent second order rate of inactivation of 2.0 ±.01 $M^{-1}s^{-1}$. This data is shown with standard error where n=6.

This rate of inactivation is lower than those observed for SHP2 and H_2O_2 (14.2 $M^{-1}s^{-1}$) and SHP2 and peroxymonocarbonate (117.88 $M^{-1}s^{-1}$) (Chapter 2). However, this rate of inactivation is close to that observed of PTP1B (3.0 ±0.5 M^{-1} s^{-1})[16] (Li,Y. unpublished data) by AITC. Both of these rates of inactivation of PTPs by AITC are comparable to those reported for H_2O_2.

Upon determining the inactivation of SHP2 by AITC, the kinetics of inactivation of SHP2 with another ITC (sulforaphane) was carried out to determine if the structure of the inactivator affected its activity against PTPs. Sulforaphane was investigated since it is the most prominent ITC found in broccoli and therefore, widely consumed. We found that sulforaphane is also a time-and concentration-dependent inactivator of SHP2 as can be seen in Figure 3.3.

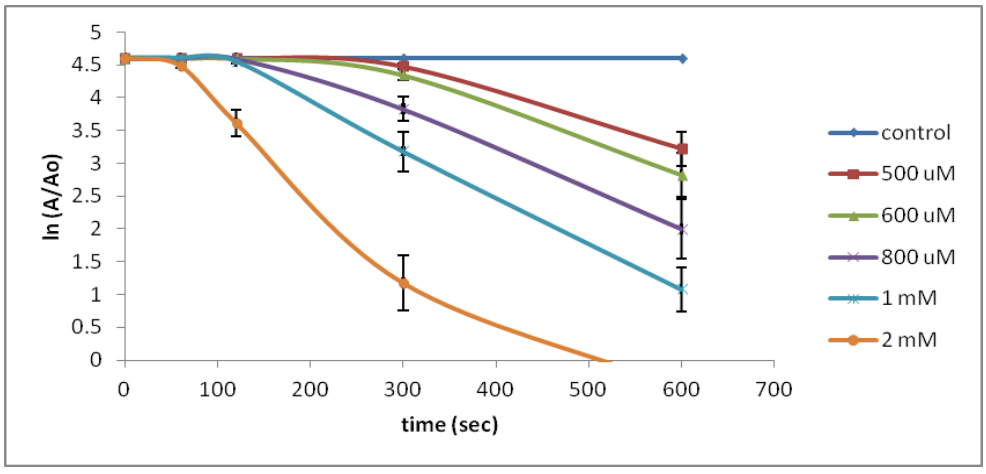

Figure 3.3 Inactivation of SHP2 in the presence of various concentrations of sulforaphane where n=4

The pseudo-first-order rate of inactivation was calculated utilizing the slopes seen in Figure 3.3 and these values were plotted against the sulforaphane concentration to give the apparent second order rate. As evident in Figure 3.4, sulforaphane inactivates SHP2 with an apparent second-order rate of $4.158 \pm 0.002 M^{-1}s^{-1}$.

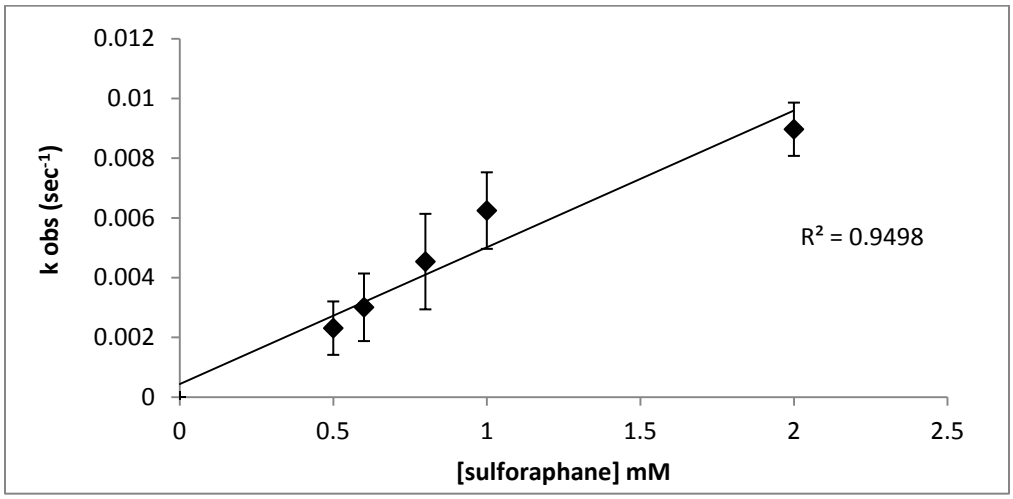

Figure 3.4 The apparent second order rate of inactivation for PTP-SHP2 by sulforaphane was calculated to be 4.518±.002 M^{-1} s^{-1}. Points represent the mean with standard error calculated where n=4.

This rate of inactivation is slightly higher than that observed for inactivation of PTP1B by sulforaphane (1.0 ± 0.1 $M^{-1}s^{-1}$)[16](Li,Y. unpublished data). This rate is also comparable to the inactivation of SHP2 by H_2O_2. In order to determine the mechanism of inactivation of SHP2, further studies were carried out utilizing both AITC and sulforaphane.

3.4 Inactivation by Isothiocyanates is Active Site Directed

Phosphate a competitive inhibitor for PTPs, and this property was utilized to determine if inactivation of SHP2 is active site directed (Scheme 3.4), as was observed for PTP1B.[16] Although Scheme 3.5 depicts the use of sulforaphane as the inactivator, AITC was also used.

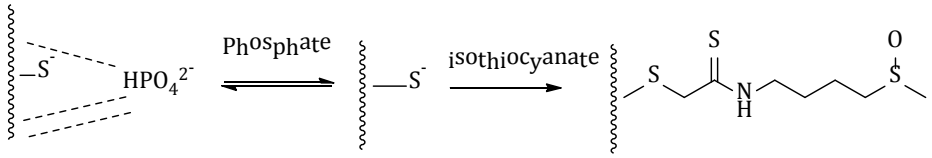

Scheme 3.6 The active site directed experiments compare the inactivation of SHP2 by ITCs alone and the inactivation by ITCs in the presence of PTPs natural substrate, phosphate.

Inactivation of SHP2 by AITC was slowed by presence of 50 mM phosphate compared to the inactivation of SHP2 by ITCs alone, which can be seen in Figures 3.5 and 3.6. This provided evidence that the inactivation of SHP2 involves interaction of AITC at the active site cysteine. This decrease in inactivation rate was also observed for PTP1B in the presence of arsenate.[16]

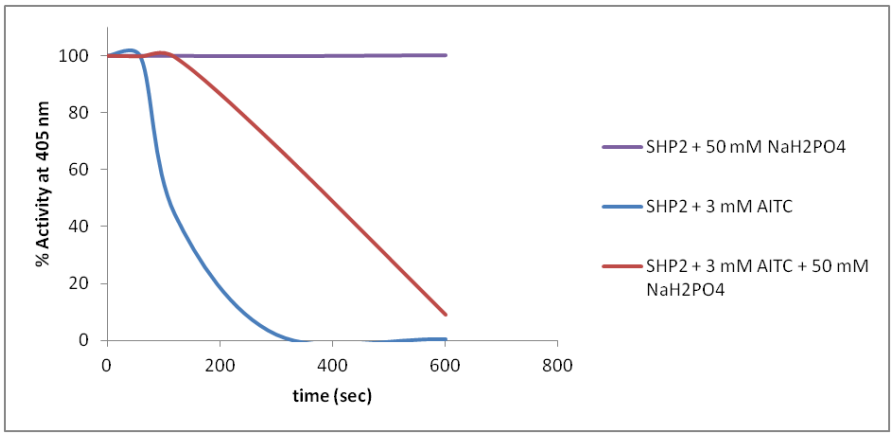

Figure 3.5 Inactivation of SHP2 by allyl isothiocyanate is slowed by the presence of 50 mM NaH_2PO_4.

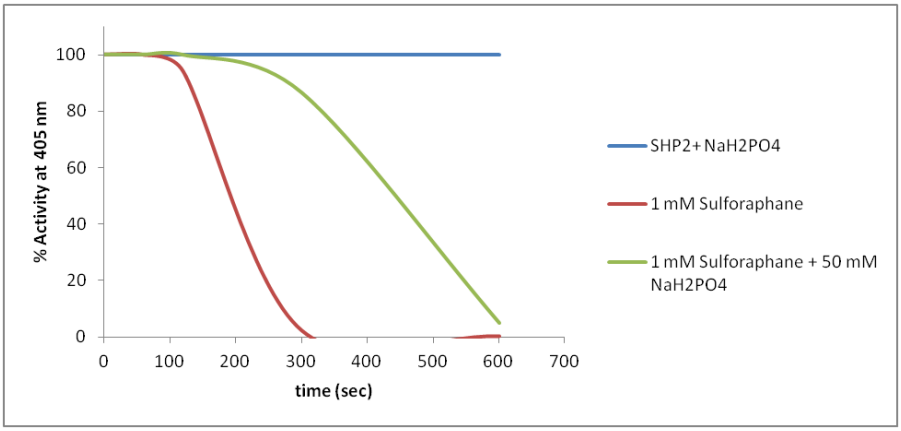

Figure 3.6 Inactivation of SHP2 by sulforaphane is slowed in the presence of NaH_2PO_4.

3.5 Discussion and Conclusion

Dietary isothiocyanates are time- and concentration- dependent inacitvators of SHP2. The rate of inactivation of allyl isothiocyanates is 2.04 ± .14 M^{-1} s^{-1} and the rate of inactivation observed for sulforaphane is 4.158 ± .002$M^{-1}s^{-1}$. The apparent second-order rate of inactivation of SHP2 by dietary isothiocyanates is comparable to those observed for PTP1B.[16] (Li, Y. unpublished data) This inactivation is slowed in the presence of phosphate and confirms the data observed for PTP1B which illustrates ITCs are active site directed[16] (Scheme 3.7).

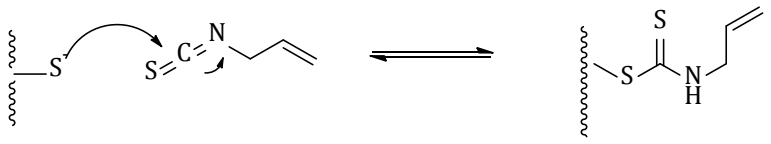

Scheme 3. 7 Proposed mechanism of active site directed inactivation of PTP by ITC.

With these data, it is apparent that although ITCs are capable to aid in the regulation of PTPs, the ITCs are not selective, and thus, will not be viable as drug precursors. ITCs have an observed 100-200 fold accumulation in the cells over 3 hours.[9] Although their control is not selective, our findings present a plausible explanation for the control of PTPs biological activity. Further research needs to focus on controlling PTPs, since they have the ability to affect many cellular mechanisms.[29-32]

3.6 Materials and Methods

3.6.1 Chemicals and Reagents

Reagents were purchased from the following suppliers: Buffer salts, *p*-nitrophenylphosphate (pNPP), thiols, ampicillin, chloramphenical, Luria Broth Media, Isopropylβ-D-1-thiogalactopyranoside, DL-Dithiothreitol, Diethylenetriaminepentaacetic acid (DTPA), Deoxyribobuclease I bovine, Kanamycin disulfide salt, Imidazole, HEPES, Allyl isothiocyanate, Sulforaphane, and Sodium Acetate (99+%) were obtained from Sigma-Aldrich (St.Louis MO). Zeba mini and micro centrifugal buffer exchange columns (catalog number 89882) and Surfact-Amps 80 (Tween), 10% solution, catalog number 28328) were obtained from Pierce Biotechnology (Rockford,IL). Restriction endonucleases *EcoRI* (catalog number R0101) and SmaI (catalog number R0141) were obtained from New England Biolabs(Ipswich, MA). BL21 DE3 compotent cells (catalog number 11665-015) were obtained from Invitrogen (Carlsbad, CA). Overnight Express Autoinduction System 1 Kit (catalog number 71300-4) was purchased from Novagen (Madison, WI). Sodium Chloride (catalog number S271), and Sodium Phosphate Monobasic (catalog number S397) were obtained from Fisher Chemicals (Fair Lawn, NJ).

3.6.2 Recombinant Expression of PTP-SHP2

DNA coding for the His-tagged catalytic subunit of SHP2 was amplified from plasmid obtained from Structural Genomics Center. The resulting construct was purified using a

0.8% agarose gel. The plasmid was isolated with Promeaga Wizard Plus Plasmid DNA columns.

Escherichia coli DH5α cells were transformed according to protocol with purified plasmids from amino acids 246-527 containing 36 kDa SHP2. Plasmid DNA from these DH5α cells was extracted and transformed into BL21 DE3 cells according to the manufacturer's protocol. Cells were selected on LB agar with kanamycin (30 μg/mL), a monoclonal sample from was placed into 0.5 L cultures of Luria Broth Kanamycin (30 μg/mL), and autoinduction media from Novagen's Overnight Express Autoinduction System 1 kit and grown for 22 hours at 18°C with 250 rpms until stationary phase was reached (which was determined by $A_{600} \geq 0.8$). Cells were harvested by centrifugation at 5000 x *g* for 30 minutes; the cell pellet was resuspended in 50 mL of binding buffer (50mM HEPES pH 7.0, 500mM NaCl, 5mM imidazole, and 0.5mM TCEP). The cells were then lysed by French Press in the presence of DNase (Deoxyribonuclease I bovine). The resulting lysate was centrifuged for 30 minutes at 3700 x *g*. After removal of DNA fragments (unbroken cells and debris) the resulting supernant was loaded onto a 5mL HisTrapHP column and equilibrated with additional lysis buffer. SHP2 was eluted with a 0 to 1 M linear gradient of imidazole at a rate of 2 mL/min. Two mL fractions were collected with an AKTAprime fraction collector system. These fractions were tested for activity with *p*-nitro phenyl phosphate (*p*NPP) and pooled. The pooled fractions were dialyzed into a 50 mM Tris buffer with 0.5 M NaCl, then loaded onto a 1.0 mL Q-sepharose column and eluted with a 25 mL gradient from 0 to 1 M NaCl linear gradient. Collected fractions were again tested for activity with *p*NPP, pooled and concentrated to

0.5 mg/mL total protein. Protein concentration was determined by the utilization of Beer's Law (equation 2.1):

$$A = \varepsilon bc \qquad \textbf{Equation 3.1}$$

The concentration is multiplied by the weight of SHP2 DNA (36823.59 g/mol). Once concentration was determined the resulting pool is divided into 100 µL aliquots and stored at -80°C until further use.

3.6.3 Recombinant Expression of PTP-SHP2

SHP2 was also grown and purified by Signh, H. from the Tanner group (unpublished data).

3.6.4 Time-Dependent Inactivation of PTP-SHP2 by Isothiocyanates

Inactivation kinetic assays were performed using existing group protocols.[16] Modifications of existing literature protocols[33-34] were made. Free thiols were removed from stock solutions of purified PTP-SHP2 using Zeba mini centrifugal exchange columns according to the manufacturer's protocol. The exchange buffer contained 50 mM Bis-Tris, 50 mM Tris, 1.0 mM DTPA, 100 mM NaOAc, and Tween 80 [0.05%] at pH 7.0. During the inactivation reactions, inactivators (allyl isothiocyanate or sulforaphane) were added as varying concentrations in exchange buffer to SHP2 at 30°C, (final

concentration of SHP2 ~20 nmol) final volume was 100 µL. A 10 µL aliquot was removed at various time points (1 minute, 2 minutes, 5 minutes, and 10 minutes) and placed into 490 µL of assay buffer (50 mM Bis-Tris, 100 mM NaCl, 10 mM DTPA, and 20 mM pNpp pH 6.0) at 37°C for 10 additional minutes. The enzymatic reaction was quenched with the addition of NaOH (500 µL of 2 M solution in water). The amount of p-nitrolphenolate released during the reaction was determined by UV-vis measurement of the absorbance at 25°C and 405 nm.

3.6.5 Time-Dependent Inactivation of SHP2 in the Presence of an Active Site Competitor

An aliquot of thiol free enzyme was combined with 5% DMSO solution of allyl isothicyante (3mM) or sulforaphane (1 mM) in exchange buffer (50 mM Bis-Tris, 50 mM Tris, 1.0 mM DTPA, 100 mM NaOAc, and Tween 80 [0.05%] at pH 7.0) and 50 mM NaH_2PO_4 at 30 °C, final volume was 100 µL. A 10 µL aliquot was removed at various time points (1 minute, 2 minutes, 5 minutes, and 10 minutes) and placed into 490 µL of assay buffer (50 mM Bis-Tris, 100 mM NaCl, 10 mM DTPA, and 20 mM pNpp pH 6.0) at 37°C for 10 additional minutes. The enzymatic reaction was quenched with the addition of NaOH (500 µL of 2 M solution in water). The amount of p-nitrolphenolate released during the reaction was determined by UV-vis measurement of the absorbance at 25°C and 405 nm.

3.7 References

(1) Xiao, D.; Srivastava, S. K.; Lew, K. L.; Zeng, Y.; Hershberger, P.; Johnson, C. S.; Trump, D. L.; Singh, S. V. *Carcinogenesis* **2003**, *24*, 891.

(2) Bones, A. M. R., John T. *Physiologia Plantarum* **1996**, *97*, 194.

(3) Musk, S. R. R.; Smith, T. K.; Johnson, I. T. *Mutation Research Letters* **1995**, *348*, 19.

(4) Munday, R.; Munday, C. M. *Journal of Agricultural and Food Chemistry* **2004**, *52*, 1867.

(5) Rouzaud, G.; Young, S. A.; Duncan, A. J. *Cancer Epidemiology Biomarkers & Prevention* **2004**, *13*, 125.

(6) Smith, T. K.; Lund, E. K.; Parker, M. L.; Clarke, R. G.; Johnson, I. T. *Carcinogenesis* **2004**, *25*, 1409.

(7) Gamet-Payrastre, L. *Current Cancer Drug Targets* **2006**, *6*, 135.

(8) NAIR, S.; LI, W.; KONG, A.-N. T. *Acta Pharmacologica Sinica* **2007**, *28*, 459.

(9) Zhang, Y.; Li, J.; Tang, L. *Free Radical Biology and Medicine* **2005**, *38*, 70.

(10) Zhang, Y. *Mutation Research/Fundamental and Molecular Mechanisms of Mutagenesis* **2004**, *555*, 173.

(11) Juge, N.; Mithen, R.; Traka, M. *Cellular and Molecular Life Sciences* **2007**, *64*, 1105.

(12) Zhang, Y.; Talalay, P.; Cho, C. G.; Posner, G. H. *Proceedings of the National Academy of Sciences* **1992**, *89*, 2399.

(13) Fahey, J. W. Z., Yuesheng; Talalay, Paul *Proceedings of the National Academy of Sciences U.S.A.* **1997**, *94*, 10367.

(14) Tian, Q.; Rosselot, R. A.; Schwartz, S. J. *Analytical Biochemistry* **2005**, *343*, 93.

(15) Fahey, J. W. Z., Amy; Talalay, Paul *Phytochemistry* **2000**, *56*, 5.

(16) Seiner, D. R., Missouri, 2009.

(17) Nho, C. W.; Jeffery, E. *Toxicology and Applied Pharmacology* **2001**, *174*, 146.

(18) Zhang, Y.; Talalay, P. *Cancer Research* **1998**, *58*, 4632.

(19) Gamet-Payrastre, L.; Li, P.; Lumeau, S.; Cassar, G.; Dupont, M.-A.; Chevolleau, S.; Gasc, N.; Tulliez, J.; Tercé, F. *Cancer Research* **2000**, *60*, 1426.

(20) Misiewicz, I.; Skupinska, K.; Kowalska, E.; Lubinski, J.; Kasprzycka-Guttman, T. *Acta Biochim Pol* **2004**, *51*, 711.

(21) Surh, Y.-J.; Kundu, J. K.; Na, H.-K. *Planta Med* **2008**, *74*, 1526.

(22) Myzak, M. C.; Dashwood, R. H. *Cancer Letters* **2006**, *233*, 208.

(23) Eggler, A. L.; Liu, G.; Pezzuto, J. M.; van Breemen, R. B.; Mesecar, A. D. *Proc Natl Acad Sci U S A* **2005**, *102*, 10070.

(24) Yang, C. S.; Smith, T. J.; Hong, J.-Y. *Cancer Research* **1994**, *54*, 1982s.

(25) Zhang, Y.; Talalay, P. *Cancer Research* **1994**, *54*, 1976s.

(26) Zhang, Y.; Yao, S.; Li, J. *Proc Nutr Soc* **2006**, *65*, 68.

(27) Harrington, H.; Ho, K.; Ghosh, S.; Tung, K. *Theoretical Biology and Medical Modelling* **2008**, *5*, 26.

(28) Chan, G.; Kalaitzidis, D.; Neel, B. *Cancer and Metastasis Reviews* **2008**, *27*, 179.

(29) Neel, B. G.; Gu, H.; Pao, L. *Trends in Biochemical Sciences* **2003**, *28*, 284.

(30) Tonks, N. K. *Nature Reviews Molecular Cell Biology* **2006**, *7*, 833.

(31) Mohi, M. G.; Neel, B. G. *Current Opinion in Genetics & Development* **2007**, *17*, 23.

(32) Feng, G.-S. *Experimental Cell Research* **1999**, *253*, 47.

(33) Silverman, R. B. In *Methods in Enzymology*; Daniel, L. P., Ed.; Academic Press: 1995; Vol. Volume 249, p 240.

(34) Montalibet, J.; Skorey, K. I.; Kennedy, B. P. *Methods* **2005**, *35*, 2.